THE UNIVERSITY OF MANITOBA

LIBRARY

AUTHOR Barbetti, Michael Francix

TITLE Pulse shape discrimination with sodium iodide

THESIS M.Sc. Univ. of Manitoba, 1968

I, the undersigned, agree to refrain from producing, or reproducing, the above-named work, or any part thereof, in any material form, without the written consent of the author:

PULSE SHAPE DISCRIMINATION WITH SODIUM IODIDE

A Thesis

Submitted to

the Faculty of Graduate Studies

University of Manitoba

In Partial Fulfillment

of the Requirements for the Degree

MASTER OF SCIENCE

by

Michael Francis Barbetti

August 1968

ACKNOWLEDGEMENTS.

The author wishes to express his gratitude to his supervisor, Dr. S. Standil, for his help and encouragement during this work.

Thanks are also due to Mr. R. Shabaga for constructing the circuit, and to Mr. G. Knote for his interest and suggestions on the electronic problems.

It is a pleasure to thank Dr. W. R. Wall for providing the data on the pulse shapes from NaI(Tl). Thanks are also due to Dr. I. F. Bubb for the loan of the Cf^{252} source, and to Dr. D. O. Wells of the cyclotron group for his co-operation.

Acknowledgement is made to the National Research Council of Canada for financial support of this research.

ABSTRACT

A pulse shape discriminator was used in conjunction with a NaI(Tl) scintillator in an attempt to identify the radiation responsible for the scintillation. The response of the discriminator to alpha- and gamma-induced pulses was determined using an Am^{241} alpha source and a Co^{56} gamma source. An attempt was also made to distinguish between neutron- and gamma-induced pulses, but this was not successful. The thesis contains a discussion of the technical problems involved in pulse shape discrimination with NaI(Tl).

TABLE OF CONTENTS

LIST OF FIGURES

CHAPTER I

INTRODUCTION

In many nuclear physics experiments different reactions occur simultaneously, often resulting in mixed spectra of more than one type of particle. To interpret these complex spectra often requires using a detection system which not only measures energy, but also identifies the different particles.

Charged particle identification systems depend on differences in the rates of energy loss in an absorber for different particles with the same energy. Information on the rate of energy loss is contained in the pulse shape from most detectors; or, alternatively, this information can be obtained by introducing a thin counter in front of the main counter in a telescope arrangement.

The various methods which have been used to extract this information from scintillation pulses, and identify the particle, are discussed in this chapter.

1.1 Two Counter Methods

A thin transmission particle detector ($\frac{dE}{dx}$ counter) placed in front of a thick detector (E counter) allows the simultaneous determination of both the rate of energy loss and the total energy. With suitable electronic processing of these two pulses, the incident particle can be identified. Two processing techniques have been widely used.

1.1.1 Slow Energy Dependence of $E.\frac{dE}{dx}$

For non-relativistic charged particles, the rate of energy loss in an absorber is given by the Bethe formula

$$\frac{dE}{dx} = K_1 \frac{MZ^2}{E} \ln K_2 \cdot \frac{E}{M}$$

where K_1 and K_2 are constants; and E, M, Z are the energy, mass, and charge number of the particle.
Since the logarithmic term varies slowly with energy this equation may be rewritten

$$E.\frac{dE}{dx} \approx K_3 MZ^2 .$$

In the early particle identifiers, such as that described by Wolfe, Silverman, and DeWire (1955), E and $\frac{dE}{dx}$ were measured separately and electronically multiplied, thus determining the value of MZ^2 and identifying the particle. However, this method has at least two limitations. Firstly, the variation of the logarithmic term is neglected and, secondly, it has been assumed that the $\frac{dE}{dx}$ counter absorbs only a very small fraction of the total energy of the particle.

Despite these limitations, identifiers based on the slow energy dependence of the product $E.\frac{dE}{dx}$ were quite useful over limited energy ranges. Various methods have been used to partially correct for these limitations, but they are at best a poor approximation.

1.1.2 Energy Invariance of $(E + \Delta E)^{\mu} - E^{\mu}$ for a given type of Particle.

A better method of particle identification, introduced by Goulding, Landis, Cerny, and Pehl (1964), is based on the observation that the range-energy relationship for charged particles with energies from 10Mev. to 100Mev. can be represented quite closely by a power law of the form

$$R = \frac{1}{k} E^{\mu} ,$$

where $\mu \approx 1.7$, depending on the absorbing material, and $k \propto M^{\mu-1} Z^{2}$. For a charged particle passing through a thin detector (ΔE detector) of thickness T and then coming to rest a distance x inside a similar thick E detector,

$$(T + x) = \frac{1}{k} (E + \Delta E)^{\mu} ,$$

while for the E detector alone,

$$x = \frac{1}{k} E^{\mu} .$$

Combining these two equations,

$$Tk = (E + \Delta E)^{\mu} - E^{\mu} = P.$$

Thus, within the limits of the power law approximation, P is dependent only on the thickness of the ΔE detector and the type of particle.

The critical part of a system for electronically

measuring the quantity P is in designing appropriate fast, accurate function generators. The function generators used by Goulding, Landis, Cerny, and Pehl (1964) and by Chaminade, Faivre, and Pain (1967) were based on the use of logarithmic function generators. This method involves generating the logarithm, multiplying electronically by μ, and generating the anti-logarithm of the pulse. Recently, Turos and Zieminski (1966) have designed a simpler diode function generator, whose output is proportional to the input raised to a certain power.

This type of particle identification system with two counters is useful only for charged particles; it cannot be used to identify neutral particles.

1.2 Pulse Shape Discrimination

Many scintillators exhibit differences in pulse shapes corresponding to different ionizing particles, while the shapes of these pulses are nearly independent of energy. Some of the better known pulse shapes are shown in Fig. 1.

For most organic scintillators, a Compton or pair-production electron scintillation differs from a proton recoil scintillation in that it contains relatively more light in the fast component (decay times $\lesssim$10 nsec.), and less light in the slow component (decay times $\gtrsim$100 nsec.).

With alkali-halide scintillators the reverse occurs. A gamma-induced scintillation and an alpha-induced scintillation differ in that the gamma-scintillation contains relatively less light in the fast components, and more

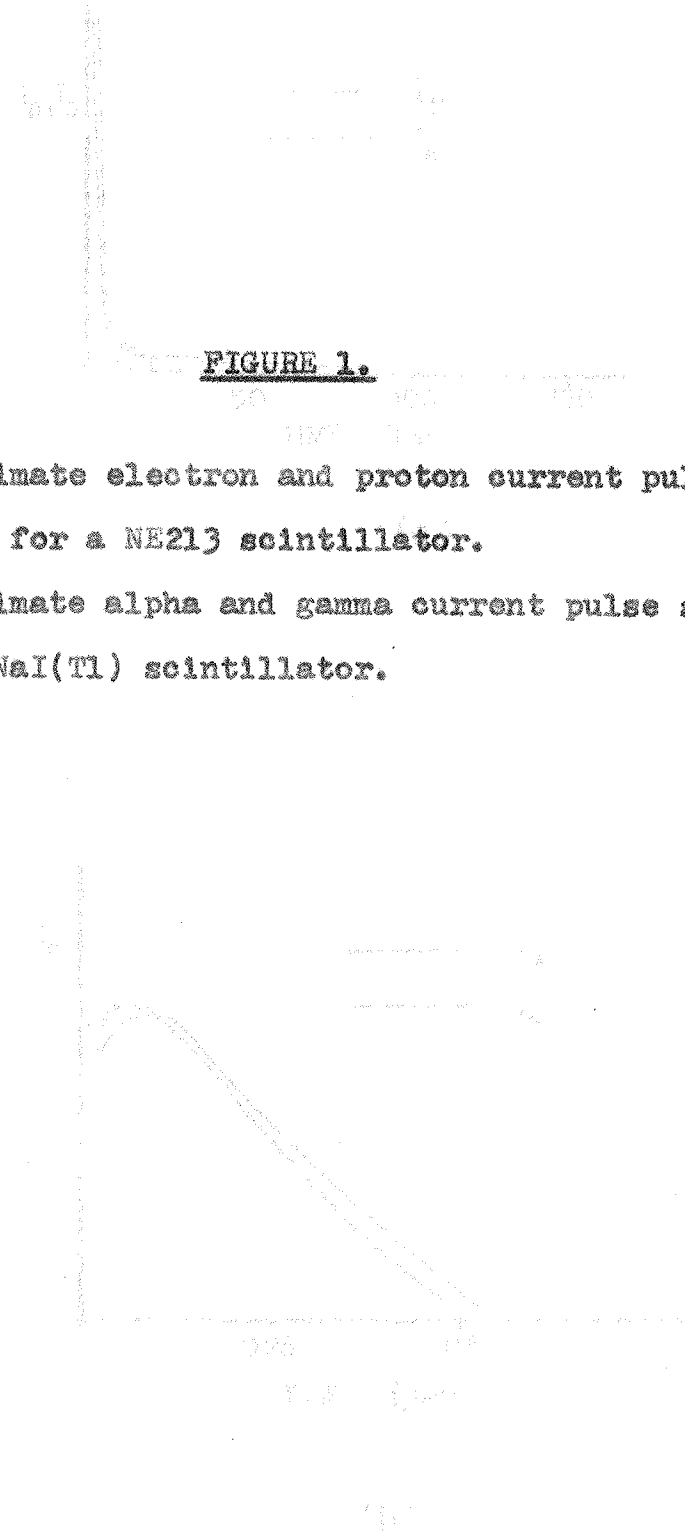

FIGURE 1.

(a) Approximate electron and proton current pulse shapes for a NE213 scintillator.

(b) Approximate alpha and gamma current pulse shapes for a NaI(Tl) scintillator.

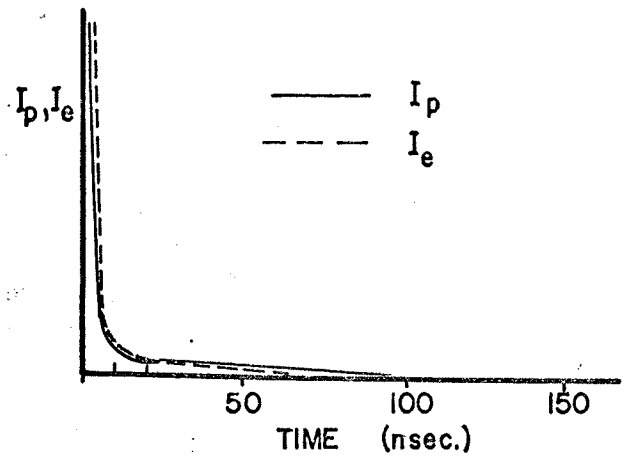
I_p, I_e
I_p
I_e
50
100
150
TIME (nsec.)

(a)

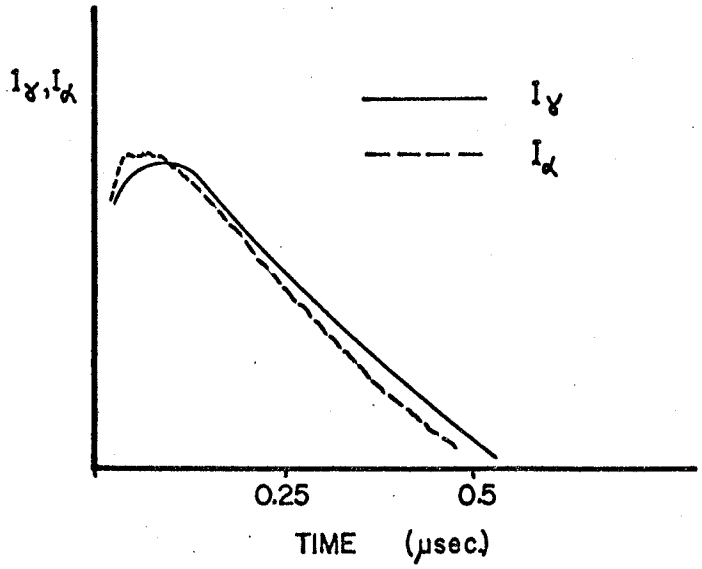
I_γ, I_α
I_γ
I_α
0.25
0.5
TIME (μsec.)

(b)

light in the slower components. Proton-induced scintillations are intermediate. CsI(Tl) exhibits larger differences in pulse shapes than NaI(Tl) and is also better for energy measurement.

Two different techniques have been developed to make use of this information to discriminate between particles.

1.2.1 Charge-Comparison Methods

Brooks (1956) calculated that a comparison of the peak height with the total area of the pulse could be used to discriminate between neutron-induced and gamma-induced pulses in an organic scintillator.

In the circuit used by Brooks, Pringle, and Funt (1960) (fig. 2(a)), the fast component is sampled at the anode with time constant R_1C_1; the capacitor C_1 is charged until the phototube current starts to fall off, thus producing a smaller voltage across R_1 than across C_1. The diode D_1 then cuts off and the decay of C_1 is determined by the combined shunt resistance. Similarly, a longer time sample of the pulse, of opposite sign, is taken at the last dynode with time constant R_2C_2.

In the photomultiplier output circuit of fig. 2(a) the anode time constant was 10 nsec., and so the amplitude of the negative pulse generated across the anode load was approximately proportional to the amount of fast component in the scintillation pulse. At the last dynode the time constant was approximately 100 nsec., and so the positive pulse amplitude produced was approximately proportional to the sum of the amounts of fast and slow components. The anode and dynode

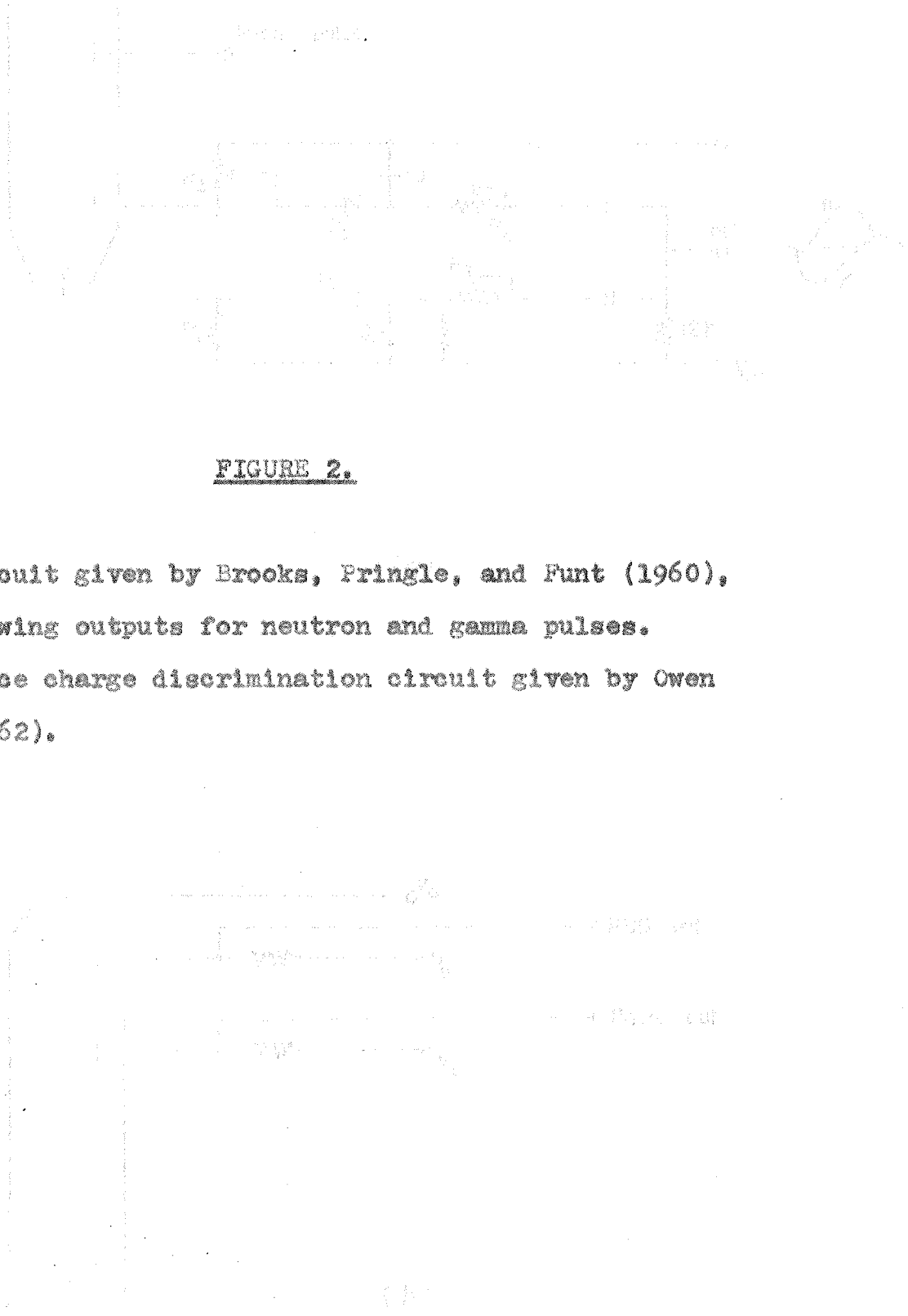

FIGURE 2.

(a) Circuit given by Brooks, Pringle, and Funt (1960), showing outputs for neutron and gamma pulses.

(b) Space charge discrimination circuit given by Owen (1962).

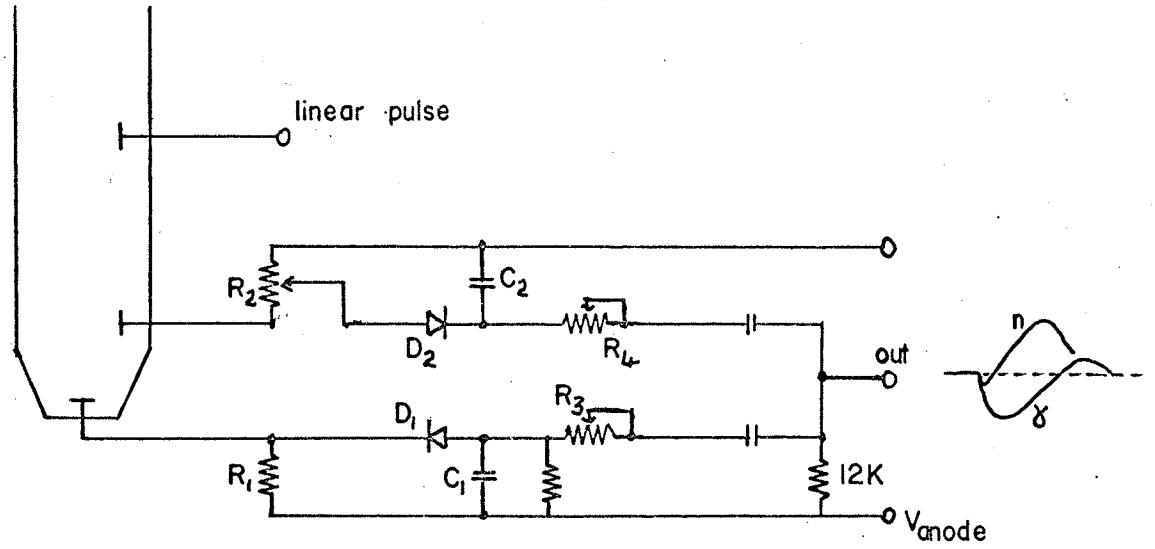
linear pulse
R2
C2
D2
R4
out
n
γ
R3
D1
R1
C1
12K
Vanode

(a)

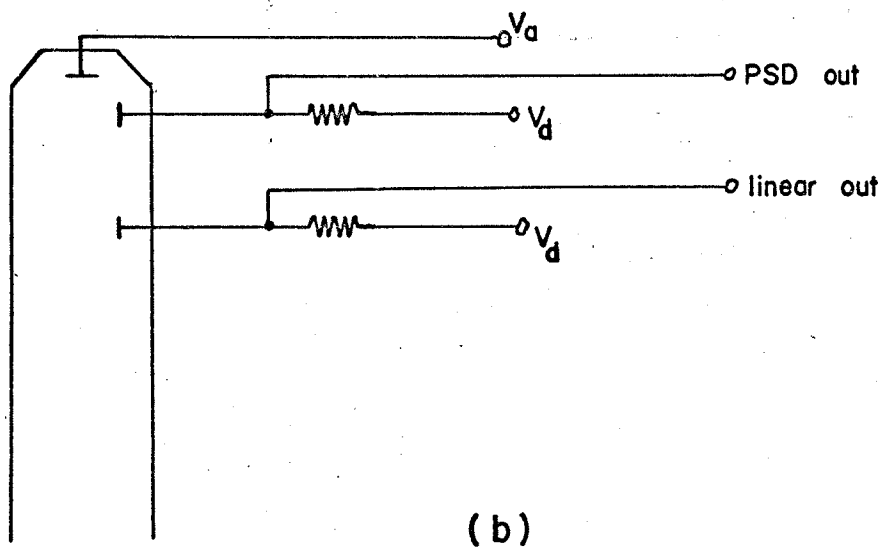
Va
PSD out
Vd
linear out
Vd

(b)

pulses were stretched and passed through variable attenuators R_3 and R_4 to the output terminal where they were mixed. The outputs for neutron and gamma scintillations are shown in Fig. 2(a).

The difficulties associated with this system were those of precisely balancing the time constants. This is particularly difficult if the potentials across the diodes are small due to the large storage capacitors C_1 and C_2. Improper adjustment results in positive overshoot in the output pulse for an electron scintillation (see fig. 2(a)). Some improvement is obtained if the positive swing at the output is required, by a coincidence gate, to arrive within a limited time from the start of the scintillation pulse. This technique has been used by Batchelor, Purnell, and Towle (1960), and by Brooks, Pringle, and Funt (1960).

In the circuit given by Jones (1968), one input pulse is sampled by both an integrating amplifier and a stretching amplifier, and the outputs are analysed by a difference amplifier to determine the relative amounts of charge in the fast and slow components. Adjustments in this circuit are not critical, and the problem of positive overshoot is avoided by resetting the amplifiers once the output of the difference amplifier has been measured, thus eliminating the necessity of balancing exactly the long decay times of the integrating and stretching amplifiers.

Owen (1958) first suggested using space charge effects in the photomultiplier as a means of particle identification.

A simple circuit given by Owen (1962) is shown in Fig. 2(b). The anode of the phototube is maintained at very nearly the potential of the last dynode. Space charge accumulation at the peak of the pulse prevents the last dynode from operating until the later stages of the pulse. The anode potential V_A is adjusted until a positive overswing is obtained only on the pulse with the longer decay time. This method can be further improved if the positive swing, which may occur for higher energy gamma-rays, is required by a coincidence gate to arrive within a limited time from the start of the scintillation pulse (Batchelor, Gilboy, and Towle (1960); and Hiramoto, Noda, and Mizutani (1967)). Hiramoto, Noda, and Mizutani (1967) and Hiramoto and Nohara (1968) have described the effect of including a shunt capacitor across the last dynode resistor. With these additions, good discrimination can be obtained between neutrons and gamma-rays using suitable organic scintillators. However, this method is not well suited for use with alkali halide crystals since it preferentially selects the longer decay time pulses, which are the gamma-ray pulses in alkali halides, and these are not usually the pulses required.

There are a number of other methods of selecting the early part of the pulse and comparing it with the later part of the pulse. Delay line clipping has been used by Forte (1959), while a method using differentiating CR circuits has been described by Forte, Konsta, and Maranzana (1961).

An accurate pulse shape discriminator with a wide dynamic range has been described by Sabbah and Suhami (1968). The positive input pulse is split by an LCR shaping network and two samples are taken, mixed, and integrated to give an output. Pulses from an organic scintillator gave a positive output for neutron-induced pulses and a negative output for gamma-induced pulses.†

The circuits described by Hiramoto and Nohara (1968) and by Sabbah and Suhami (1968) have given good discrimination between neutron- and gamma-induced pulses over a wide dynamic range. With these circuits it has apparently not been possible to discriminate satisfactorily between other particles where the differences in pulse shapes are minimal. The circuit given by Jones (1968) (mentioned above) should be capable of discriminating between pulse shapes where the differences are quite small.

1.2.2 Zero-crossing Methods.

A method making efficient use of the information available in the pulse shape was first used by Máthé and Schlenk (1964) and independently by Roush, Wilson, and Hornyak (1964). If the current pulse flowing in the photomultiplier is integrated at the anode, the risetime of the output pulse depends on the integrating time constant and on the shape of the current pulse. In this way, the risetime of

---

† The unit is manufactured by Elron Electronic Industries, Haifa, Israel.

the integrated output contains information on the type of particle inducing the scintillation, and measurement of the risetime of the pulses determines the identity of the particle.

The rate of emission of the photons from an excited scintillator can be described by a combination of exponential terms, each corresponding to decay from either a metastable or radiative state. The rate of emission of photons from commerical NaI(Tl) at room temperature following gamma-excitation can best be described by four exponential terms (Wall and Roulston (1968)). The time distribution function for emitted photons (excitation at t=0) is

$$n(t) = \sum_{i=1}^{4} A_i \exp(-\frac{t}{\tau_i})$$

where the A_i ($A_1 = 600$, $A_2 = 15$, $A_3 = -300$, $A_4 = -315$) determine the relative amplitudes of each component and the τ_i ($\tau_1 = 200$ nsec., $\tau_2 = 800$ nsec., $\tau_3 = 65$ nsec., $\tau_4 = 1$ nsec.,) are decay constants of excited states in the crystal. A_3 and A_4 are negative, and effect a finite risetime in the photon emission curve. Assuming each scintillation contains a large number of photons so that statistical fluctuations are small, and neglecting time-of-flight variations for electrons in the photomultiplier, the current flowing in the photomultiplier and arriving at the anode is given by

$$I(t) = \sum_{i=1}^{4} B_i \exp(-\frac{t}{\tau_i}).$$

The total charge contained in the current pulse is

$$Q = \int_0^\infty I(t)\,dt = \sum_{i=1}^{4} \int_0^\infty B_i \exp(-\frac{t}{\tau_i})\,dt = \sum_{i=1}^{4} (B_i \tau_i) = \sum_{i=1}^{4} Q_i$$

where Q_i is the charge contained in the i^{th} component,

Thus,

$$I(t) = \sum_{i=1}^{4} \frac{Q_i}{\tau_i} \exp(-\frac{t}{\tau_i})$$

At the anode, this current is integrated with time constant R_1C_1, where R_1 is the load resistor at the anode and C_1 is the total stray capacitance of the photomultiplier and the dynode chain. The voltage pulse appearing at the anode is given by

$$V(t) = \sum_{i=1}^{4} \frac{Q_i}{C_1} \cdot \frac{R_1C_1}{(\tau_i - R_1C_1)} \left[\exp(-\frac{t}{\tau_i}) - \exp(-t/R_1C_1)\right]$$

in the case where $\tau_i \neq R_1C_1$, $i = 1,\ldots,4$.

V(t) may be written as the product of an amplitude and a shape factor,

$$V(t) = \frac{Q}{C_1} v(t) = V_o \cdot v(t)$$

Substitution gives

$$v(t) = \sum_{i=1}^{4} \frac{Q_i}{Q} \cdot \frac{R_1C_1}{(\tau_i - R_1C_1)} \left[\exp(-\frac{t}{\tau_i}) - \exp(-t/R_1C_1)\right]$$

Thus, if the pulse shape is independent of energy, the risetime of the voltage pulse depends on both the integrating time constant R_1C_1 and on the relative amount of charge in each of the components.

For alkali halide scintillators, voltage pulses corresponding to gamma-induced scintillations exhibit longer risetimes than pulses corresponding to alpha-induced scintillations (fig. 3(a)), while photon pulses are intermediate. However, the risetimes are practically independent of energy, and are characteristic of the particle inducing the scintillation.

The risetime of the integrated voltage pulses can be determined by measurement of their zero-crossing time after RC differentiation. The shape of the voltage pulse after RC differentiation with time constant R_2C_2 is given by

$$V_d(t) = \sum_{i=1}^{4} \frac{Q_i}{Q} R_1C_1R_2C_2 \left[- \frac{\exp(-\frac{t}{\tau_i})}{(\tau_i - R_2C_2)(\tau_i - R_1C_1)} - \frac{\exp(-\frac{t}{R_2C_2})}{(R_2C_2 - R_1C_1)(R_2C_2 - \tau_i)} \right.$$

$$\left. - \frac{\exp(-\frac{t}{R_1C_1})}{(R_2C_2 - R_1C_1)(\tau_i - R_1C_1)} \right]$$

provided none of the time constants $\tau_1 \ldots \tau_4$, R_1C_1, R_2C_2, are equal. Thus, the zero-crossing time depends on both the integrating and differentiating time constants as well as

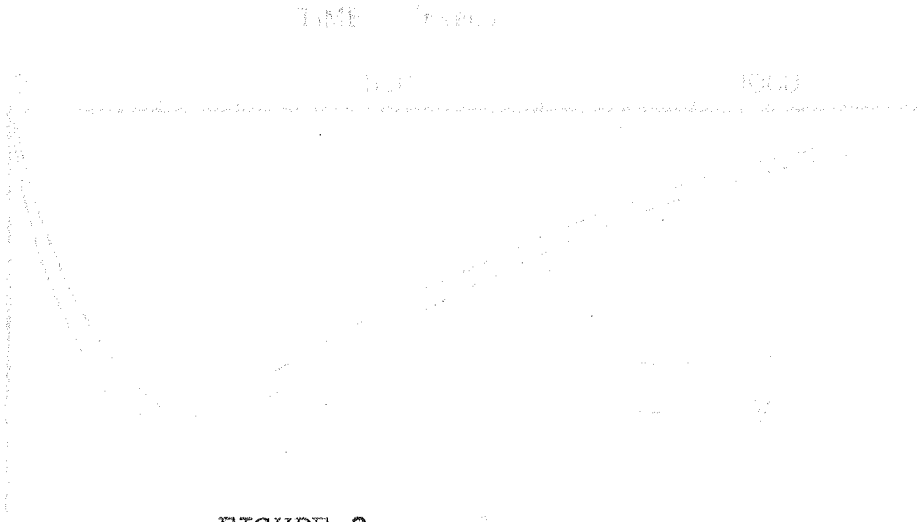

FIGURE 3.

(a) Integrated pulse shapes for alpha and gamma scintillations in NaI(Tl). Integrating time constant is 250 nsec.

(b) Differentiated pulse shapes for alpha and gamma scintillations in NaI(Tl). The integrating time constant is 250 nsec. and the differentiating time constant is 50 nsec. The gamma pulse shapes were obtained by calculation using data given by Wall and Roulston (1968). The alpha pulse shapes are approximate.

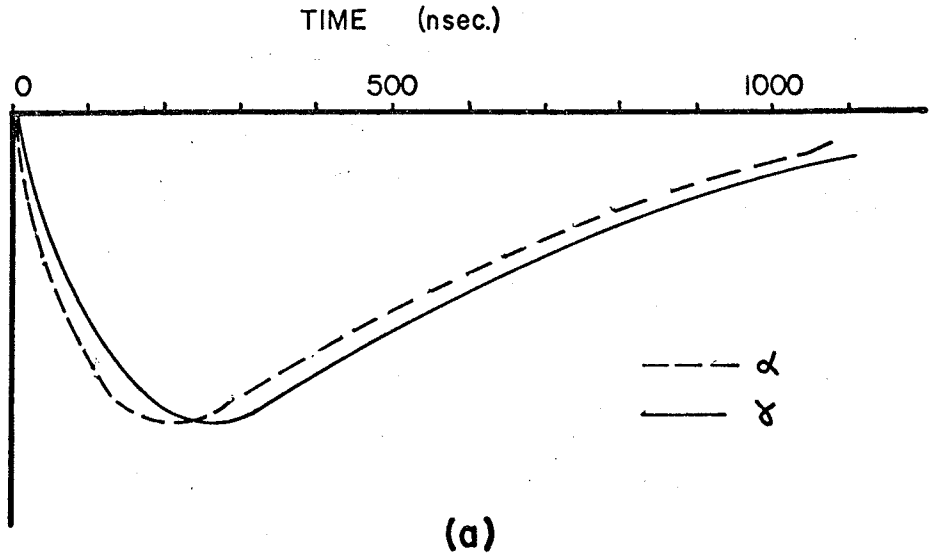

(a)

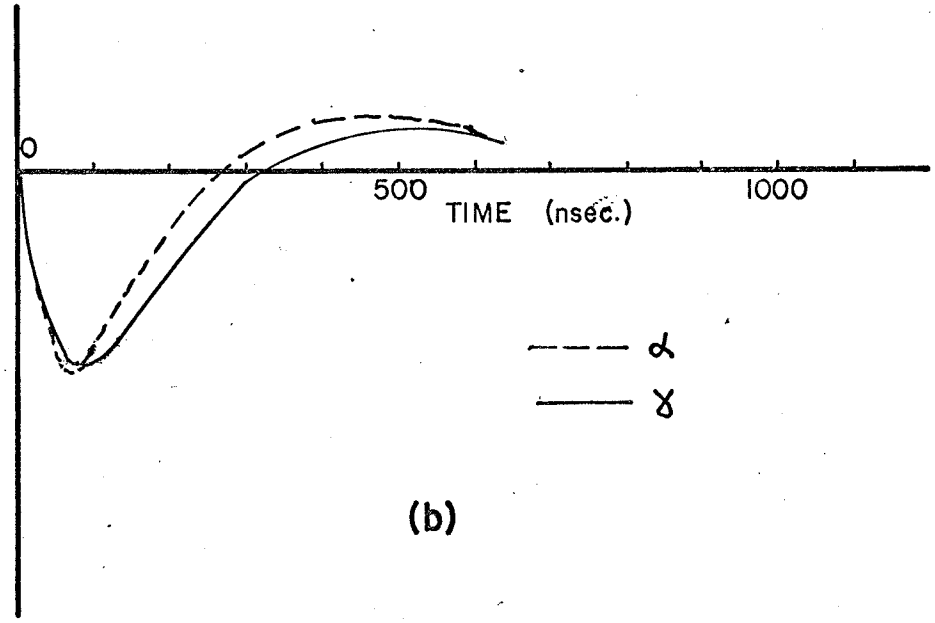

(b)

on the shape of the scintillation pulse. Pulses which have different risetimes after integration will have different zero-crossing times after differentiation (Fig. 3(b)).

Calculations have been performed by Roush, Wilson, and Hornyak (1964) and by Fülle, Máthé, and Netzband (1965) to investigate the effect of the RC time constants for integration and differentiation of the detector pulses. To obtain adequate performance of the pulse shape discrimination circuit over a wide range of pulse amplitudes requires careful consideration of small pulses. The gradual slope of the small pulses as they cross zero enhances the spread of zero-crossing times due to statistical fluctuations in the tail of the pulse. If T_1 and T_2 represent the zero-crossing times for pulses corresponding to two types of incident particles, then the ability to separate the two types of pulse depends on the magnitude of (T_2-T_1) as well as on the magnitude of the slope of the differentiated pulses at the zero-crossing points.

Roush, Wilson, and Hornyak (1964) have defined a figure-of-merit for a particular set of parameters as being the product of (T_2-T_1) with the smaller of the slopes of the differentiated pulses evaluated at T_2 and T_1. Their calculations, assuming two exponential components for NaI(Tl) (see fig. 4(b)), give essentially the same results as the calculations and experimental results of Fülle, Máthé, and Netzband (1965). Zero-crossing times of gamma-pulses, calculated by the author using the four exponential components

FIGURE 4.

(a) Zero-crossing times for gamma pulses from NaI(Tl) as a function of integrating and differentiating time constants (calculated by the author).

(b) Figure-of-merit values indicating the theoretical ability of a circuit to separate gamma and noise pulses from NaI(Tl). Dashed lines show the calculated zero-crossing times for gamma pulses (Roush, Wilson and Hornyak (1964)).

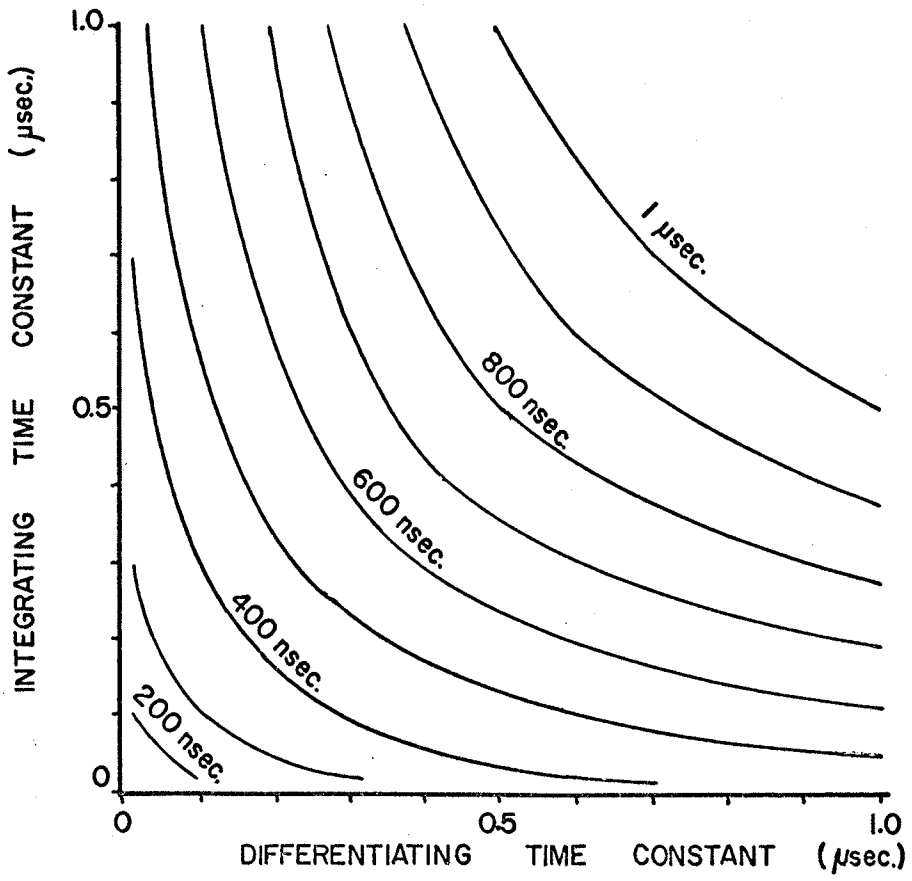
INTEGRATING TIME CONSTANT (μsec.)
1.0
0.5
0
0
0.5
1.0
DIFFERENTIATING TIME CONSTANT (μsec.)
1 μsec.
800 nsec.
600 nsec.
400 nsec.
200 nsec.

(a)

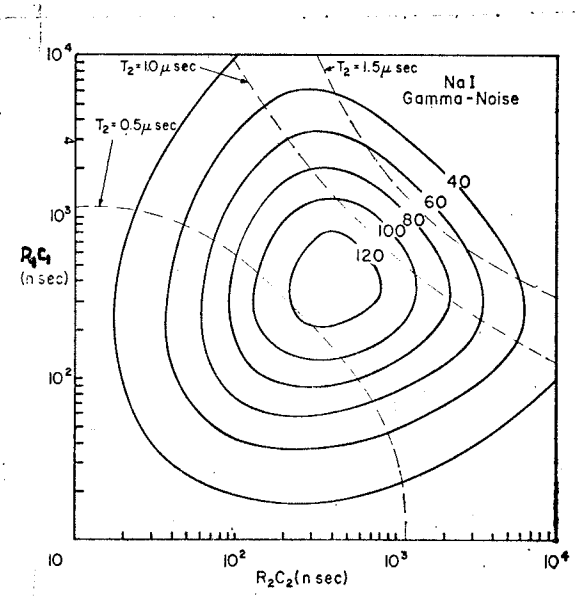
T_2 = 1.0 μ sec
T_2 = 1.5 μ sec
T_2 = 0.5 μ sec
NaI
Gamma-Noise
40
60
80
100
120
R_1C_1 (n sec)
10^4
10^3
10^2
10
10^2
10^3
10^4
R_2C_2 (n sec)

(b)

given by Wall and Roulston (1968), (see fig. 4(a)), do not differ appreciably from the results of Roush, Wilson, and Hornyak (1964), since the relative amplitudes of the two additional components are small.

Calculations and experiments with other scintillators have shown their ability to discriminate between different particles, although the optimum values of time constants are usually somewhat shorter in the case of organic scintillators. (Roush, Wilson, and Hornyak (1964); Legler, Attwenger, May, and Quittner (1965); Souček and Chase (1967); Nadav and Kaufman (1965)).

Legler, Attwenger, May and Quittner (1965) have obtained good discrimination between gamma- and neutron-induced pulses by using this method with a ^{6}LiF(ZnS) scintillation counter. In this case, the differentiated pulses show large differences in zero-crossing times, which facilitates their electronic separation. A Schmitt trigger with a small hysteresis was used as a discriminator, giving rectangular output pulses with a length corresponding to the length of the input pulse at the discrimination level. Neutron-induced pulses usually gave longer output pulses from the Schmitt trigger. However, at a given discrimination level, there were gamma-induced pulses which were large enough to give longer output pulses than small neutron-induced pulses. By means of a pulse length discriminator, all pulses shorter than a given length were suppressed, so that only neutron-induced pulses were counted.

Using scintillators where differences in pulse rise-times are minimal requires the use of more accurate electronic analysis. Roush, Wilson, and Hornyak (1964) amplified the differentiated pulses and applied the signals to a tunnel diode, which was immediately driven into its high voltage state and remained in this state until just before the zero-crossing point of the pulse. The tunnel diode provided a very stable base-line along which to measure the pulse length; this base-line was, however, maintained at a small negative voltage, giving rise to some spread in measured zero-crossing times, especially for small pulses.

Bass, Kessel, and Majoni (1964) have designed a pulse shape discriminator for use in conjunction with a double delay-line clipped amplifier. The bipolar output pulses of the amplifier are analysed in two channels: one for the positive part of the pulse, another for the negative part. Both channels have discriminators which are set so that the errors introduced by the finite triggering levels tend to cancel. The finite triggering levels eliminate small spurious pulses. A variable delay with high resolution in the first channel brings the two output pulses to coincidence for a certain risetime of the detector pulses. Appreciable discrimination between (n,p) and (n,α) reactions produced by neutrons in NaI(Tl) and KI(Tl) crystals has been obtained. The measured zero-crossing time changes somewhat with pulse amplitude, especially for small pulses, although this problem is not as serious as with the circuit of Roush, Wilson and Hornyak (1964).

The method of Fülle, Máthé, and Netzband (1965) is essentially the same as that of Bass, Kessel, and Majoni (1964), except that the outputs from the two channels are fed to a time-to-amplitude converter made up from an overlapping stage and an integrating amplifier.

A circuit using the same principle as that used by Roush, Wilson, and Hornyak (1964) has been used by Nadav and Kaufman (1965). However, this circuit is electronically much faster, and is probably capable of better separation.

The performance of the above circuits is impaired by the shift in measured zero-crossing times for small pulses. This is due to the fact that the zero-crossing time is measured along a discrimination level which is set at a small voltage. Souček and Chase (1967) have designed a circuit to reduce this source of error. The circuit incorporates three tunnel diode discriminators, one for setting an energy threshold, one for marking the leading edge of the input signals, and one for marking the zero-crossing point. The first discriminator is used to reject pulses of small amplitude which could not be measured accurately. The second and third discriminators fire on the leading edges and the zero-crossing points of the pulses, and their outputs are connected to a simple time-to-amplitude converter. This arrangement has the advantage that the second and third diodes are normally biased off. They are unbiased to the sensitive state, very near to the peak current point, only a few nanoseconds before receiving signals whose timing information is to be extracted. Good discrimination has been

obtained with this circuit used in conjunction with some organic scintillators.

Johnson (1968) has designed a circuit having two tunnel diode discriminator circuits to mark the leading edge and the zero-crossing points. The outputs from these discriminators were fed to a time-to-pulse-height converter. The circuit was adjusted to operate with a threshold of 20mv., and gave very good discrimination with pulses from a stilbene scintillator.

1.2.3 Limitations of Pulse Shape Discrimination.

Sabbah and Suhami (1968) have shown that, statistically, the charge comparison method is superior to the zero-crossing method below about 600 kev., because the zero-crossing discriminator has a finite threshold. Above 600 kev. the two methods are approximately equivalent. Their ability to discriminate between two particles is limited by statistical variations in pulse shape, by variations of pulse shape due to the superposition of small noise pulses, and by electronic variations in the circuitry.

However, the zero-crossing method is simpler to use, especially when there are more than two different types of particles present, since a simple time-to-amplitude converter can be used to generate an output pulse whose height indicates the type of particle. With charge comparison circuits, the output is not constant with energy for a given type of particle, and complex circuitry is required at the output to signal uniquely the type of particle registered.

CHAPTER II

EXPERIMENTAL

The various neutron cross sections of Na and I can be directly studied by using a NaI(Tl) scintillation crystal as a target for the incident neutrons. Since many different reactions may occur simultaneously, the study of a particular reaction requires a system which will discriminate between different reaction products. It was hoped to construct an efficient pulse shape discrimination system for NaI(Tl) scintillators, and eventually to use the available large 9 1/2" by 8 3/4" NaI(Tl) crystal for studies at neutron energies up to 45 Mev. However, this was not achieved for reasons made obvious below.

2.1 Instrumentation.

A 1" by 1 1/2" Harshaw NaI(Tl) crystal was mounted on an RCA 6342A photomultiplier operated with a non-linear dynode chain and a single stage emitter follower (see fig. 5).

The pulse shape discrimination circuits used by Johnson (1968) and by Souček and Chase (1967) gave accurate measurement of the zero-crossing time of differentiated pulses from organic scintillators. When these circuits are used with alkali halide scintillators, the walk due to the finite triggering levels of the tunnel diode discriminators becomes a serious problem, because of the slower rise and decay of the scintillation pulses.

The circuit given by Souček and Chase (1967), described in the previous chapter, seemed to be more suitable

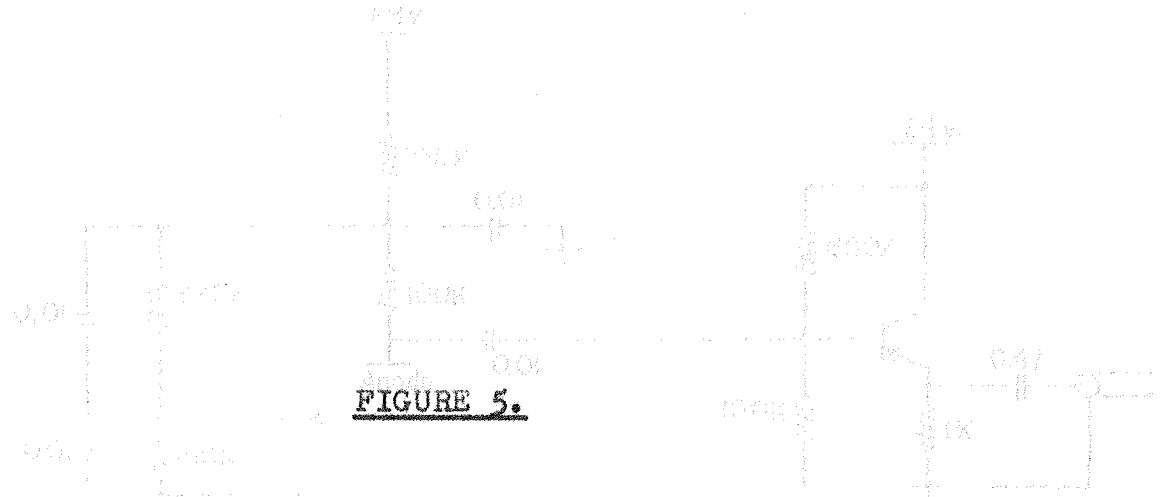

FIGURE 5.

Circuit diagram for the dynode chain and emitter follower.

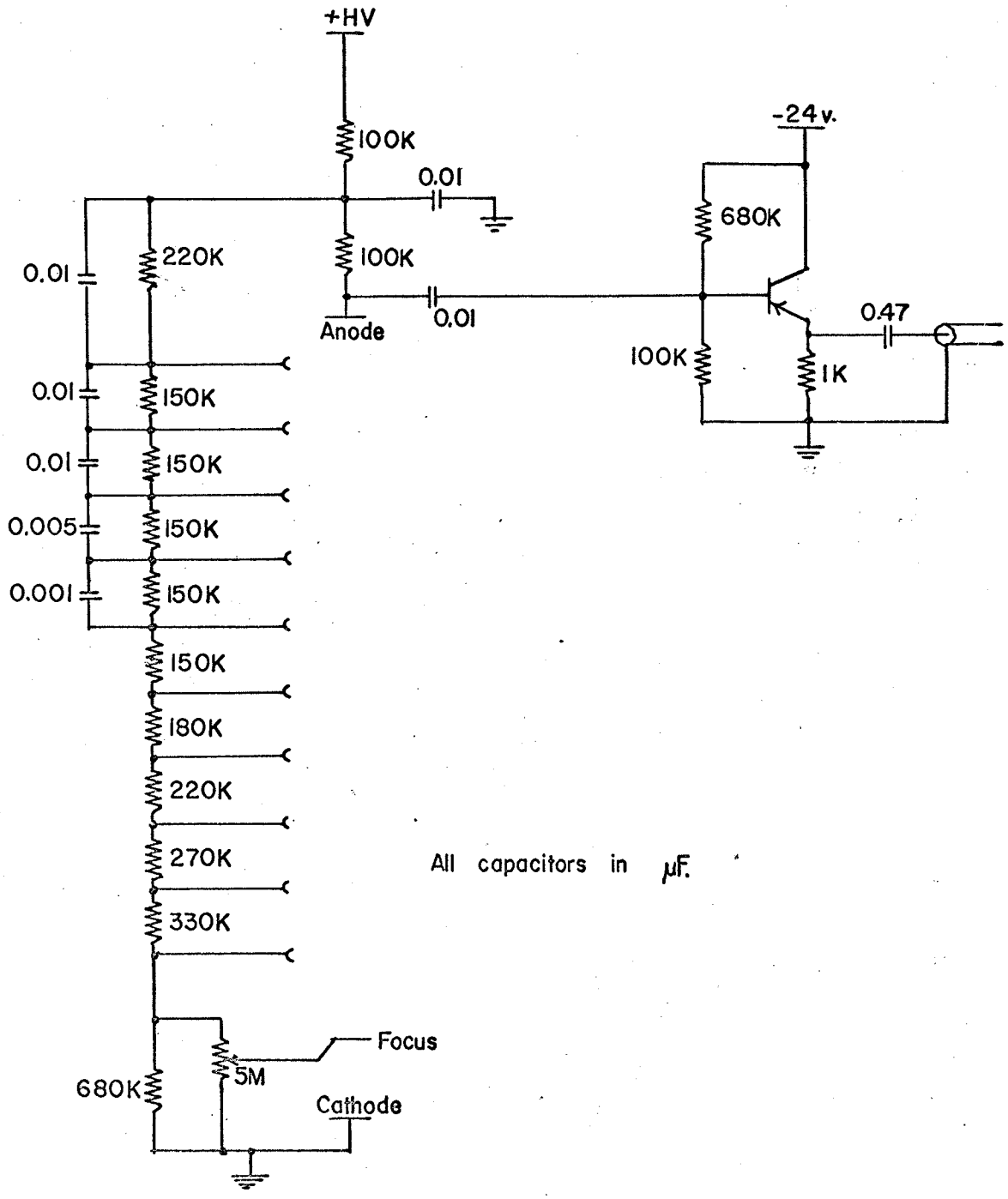
+HV
100K
0.01
220K
100K
0.01
Anode
0.01
0.01
150K
0.01
150K
0.005
150K
0.001
150K
150K
180K
220K
270K
330K
Focus
5M
680K
Cathode
-24v.
680K
0.47
100K
1K
All capacitors in μF.

for use with a NaI(Tl) crystal, since it incorporates an additional discriminator to set the threshold requirement. The circuit diagram is shown in fig. 6.

From fig. 4(b), the optimum value of both the integrating and differentiating time constants is about 0.5 μsec. However, with these time constants the slope of the differentiated pulses was small at the zero-crossing point, and walk in the measured zero-crossing time severely limited the dynamic range of the unit. It was necessary to increase the slope of the zero-crossing point and at the leading edge by decreasing the value of both time constants. The circuit was finally used with an integrating time constant of 250 nsec. at the anode, and a differentiating time constant of less than 50 nsec. in the pulse shape discriminator.

In order to calibrate the pulse shape discriminator, an Am^{241} alpha source was mounted directly over a 1/16" hole drilled in the crystal casing and a Co^{56} gamma source was placed near the crystal. The mixed energy spectrum of the sources is shown in fig. 7. The detector pulses were taken to a single channel analyser (SCA) and the pulse shape discriminator (PSD). The PSD output, gated by the SCA output, was taken to a multichannel analyser. Fig. 8 shows the output of the pulse shape discriminator for alpha and gamma input pulses of given pulse height. The output is shown as a function of pulse height rather than energy, since the changes in the measured zero-crossing time at low and at high pulse heights are instrumental, and are not due to

FIGURE 6.

Circuit diagram for the pulse shape discriminator (from Souček and Chase (1967)).

Values of the variable components used in our circuit were:

C-1	not used	L-1	100μH
C-2	50pF	L-2	100μH
C-3	470pF	L-3	100μH

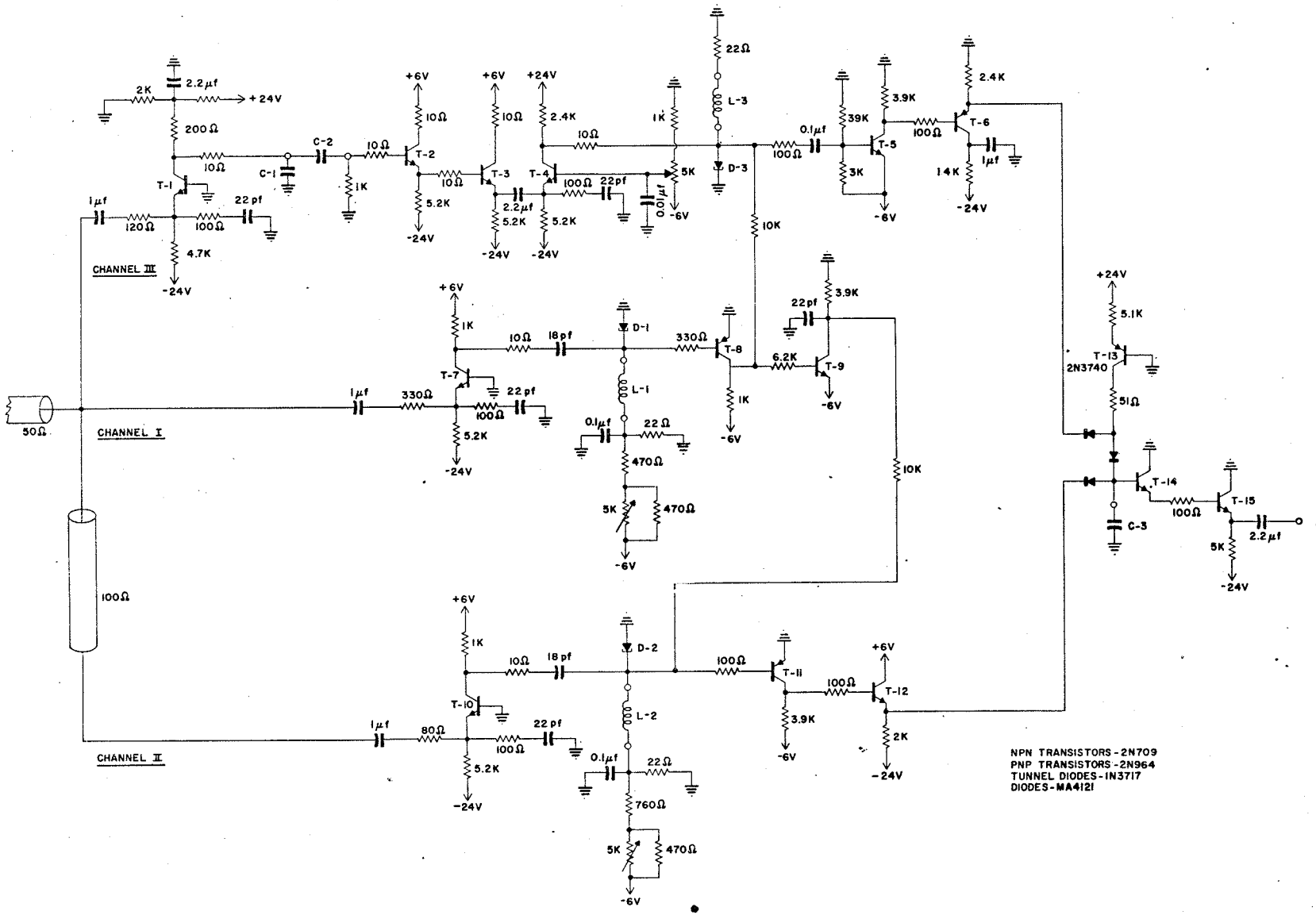
CHANNEL III
CHANNEL I
CHANNEL II
50Ω
100Ω
T-1
T-2
T-3
T-4
T-5
T-6
T-7
T-8
T-9
T-10
T-11
T-12
T-13
2N3740
T-14
T-15
D-1
D-2
D-3
L-1
L-2
L-3
C-1
C-2
C-3
+24V
+6V
-24V
-6V
2K
200Ω
10Ω
1K
5.2K
2.2μf
1μf
120Ω
100Ω
22 pf
4.7K
2.4K
22Ω
5K
0.01μf
0.1μf
39K
3K
3.9K
1.4K
10K
18 pf
330Ω
6.2K
470Ω
760Ω
80Ω
5.1K
51Ω
NPN TRANSISTORS - 2N709
PNP TRANSISTORS - 2N964
TUNNEL DIODES - IN3717
DIODES - MA4121

FIGURE 7.

Mixed energy spectrum of the Am^{241} and Co^{56} sources.

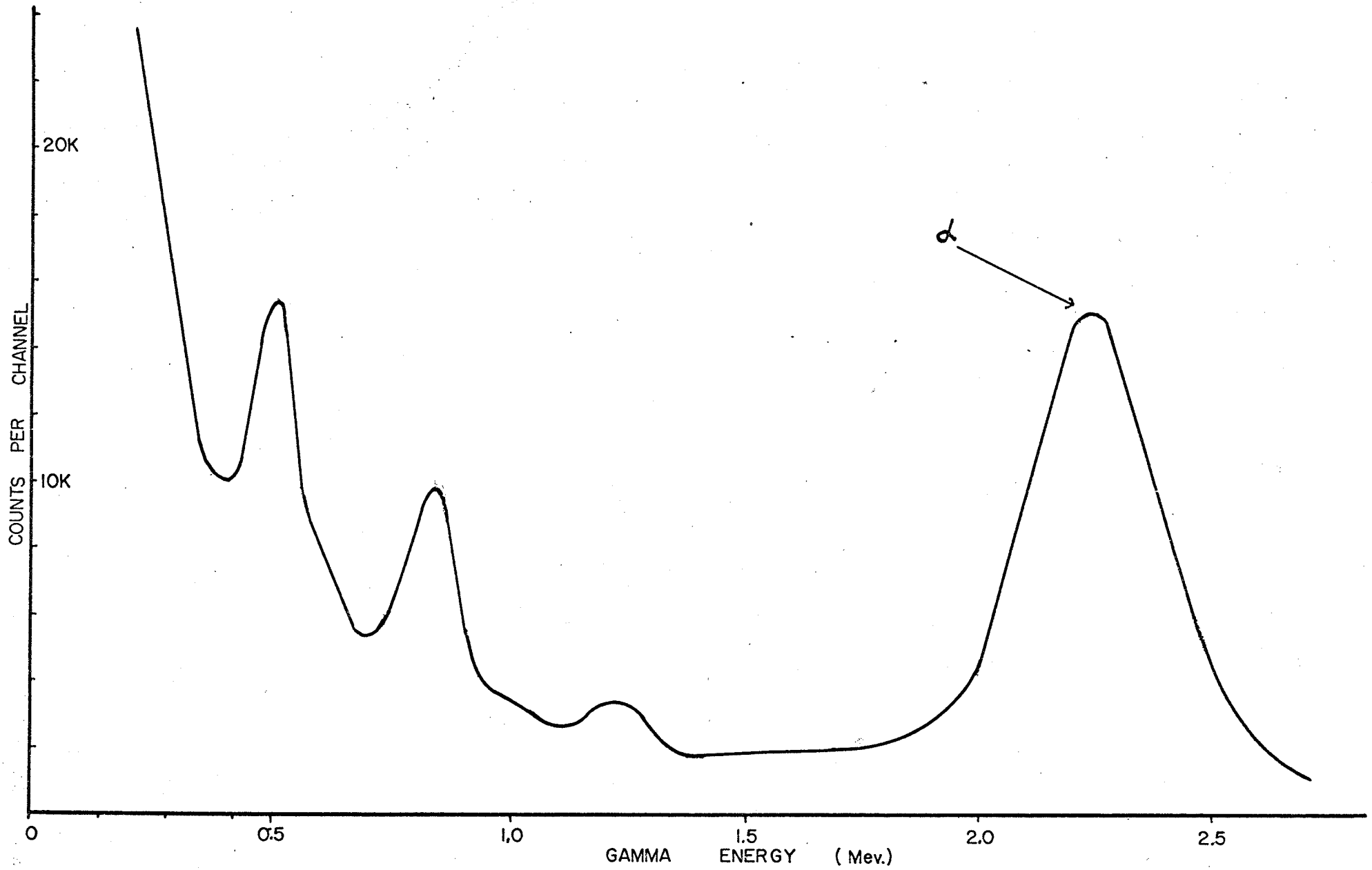
20K
10K
COUNTS PER CHANNEL
α
0
0.5
1.0
1.5
2.0
2.5
GAMMA ENERGY (Mev.)

FIGURE 8.

Output from the time-to-amplitude converter of the pulse shape discriminator for alpha- and gamma-induced pulses from NaI(Tl). The bars show the full width at half maximum for input pulses with given pulse height.

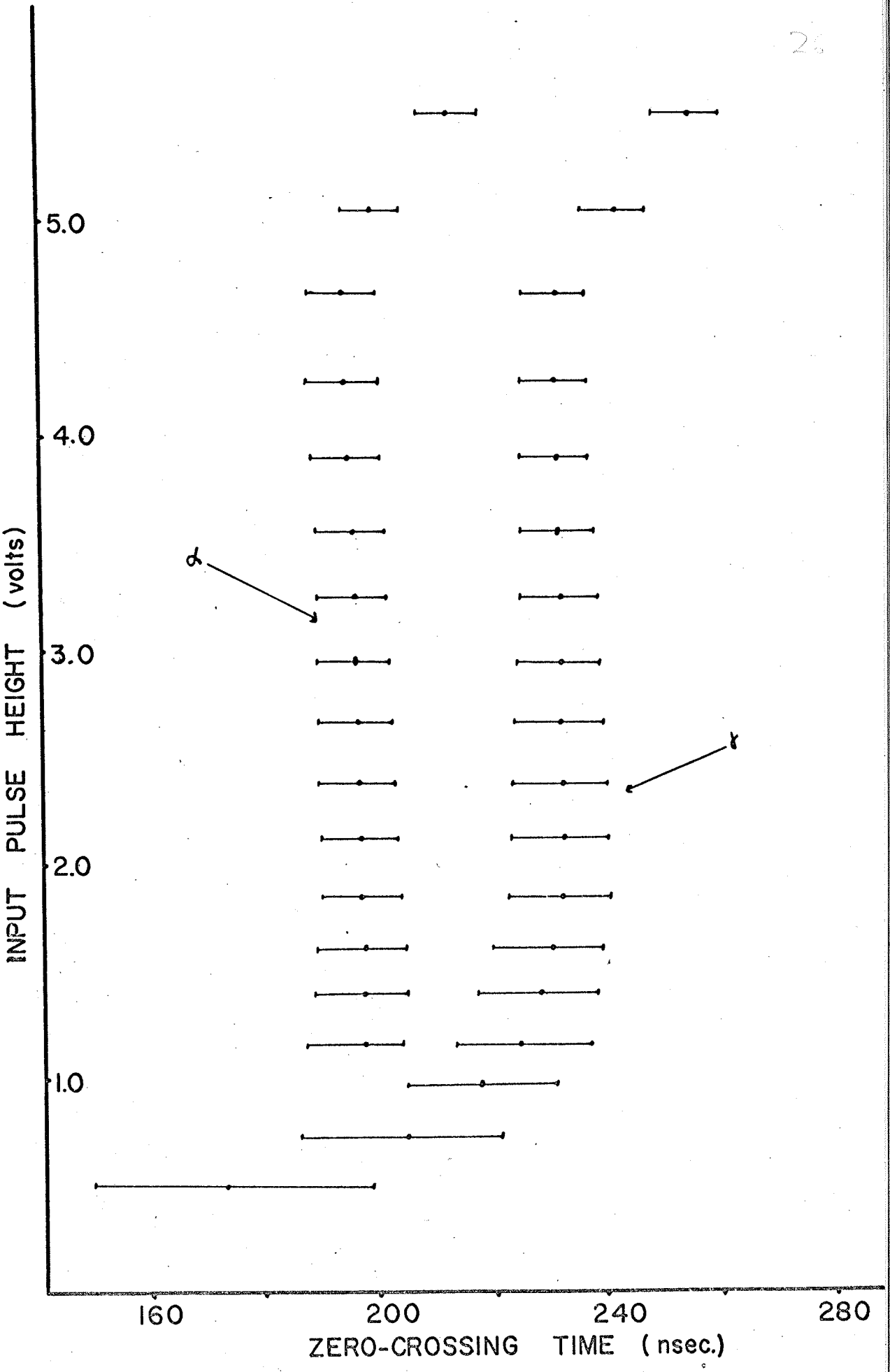
5.0
4.0
3.0
2.0
1.0
INPUT PULSE HEIGHT (volts)
α
γ
160
200
240
280
ZERO-CROSSING TIME (nsec.)

actual changes in pulse shape. The change in output above pulse heights of about 5 volts is due to limiting in the transistor amplifier T-1 preceding the differentiator. The change in output for pulse heights below 1.5 volts is caused partly by delayed and uncertain firing of the threshold tunnel diode discriminator as the pulse heights tend toward the threshold pulse height. This causes a delay in the firing of the tunnel diode discriminator marking the leading edge of the pulse.

When the high voltage applied to the phototube was increased or decreased, pulses with the same pulse height, but corresponding to a different energy, gave the same output, except that the full width at half maximum was smaller for the higher energy pulses, since statistical fluctuations in the pulse shape become less important. In this way, no significant change in the scintillation pulse shape was observed with energy, although the zero-crossing times of higher energy pulses appeared to be consistently, but not significantly shorter than lower energy pulses with the same amplitude. Such a change in pulse shape, if it exists, would be consistent with the model of Wall and Roulston (1968).

A block diagram of a spectrometer incorporating the pulse shape discriminator is shown in fig. 9. The PSD output is gated by the output from a SCA in parallel, allowing selection of PSD outputs corresponding to a given range of input pulse heights. In this way, all input pulses are received by the pulse shape discriminator, but with as little distortion as possible. The second SCA was used to select

FIGURE 9.

Block diagram of the spectrometer arrangement used to obtain an energy spectrum of pulses with given measured zero-crossing times.

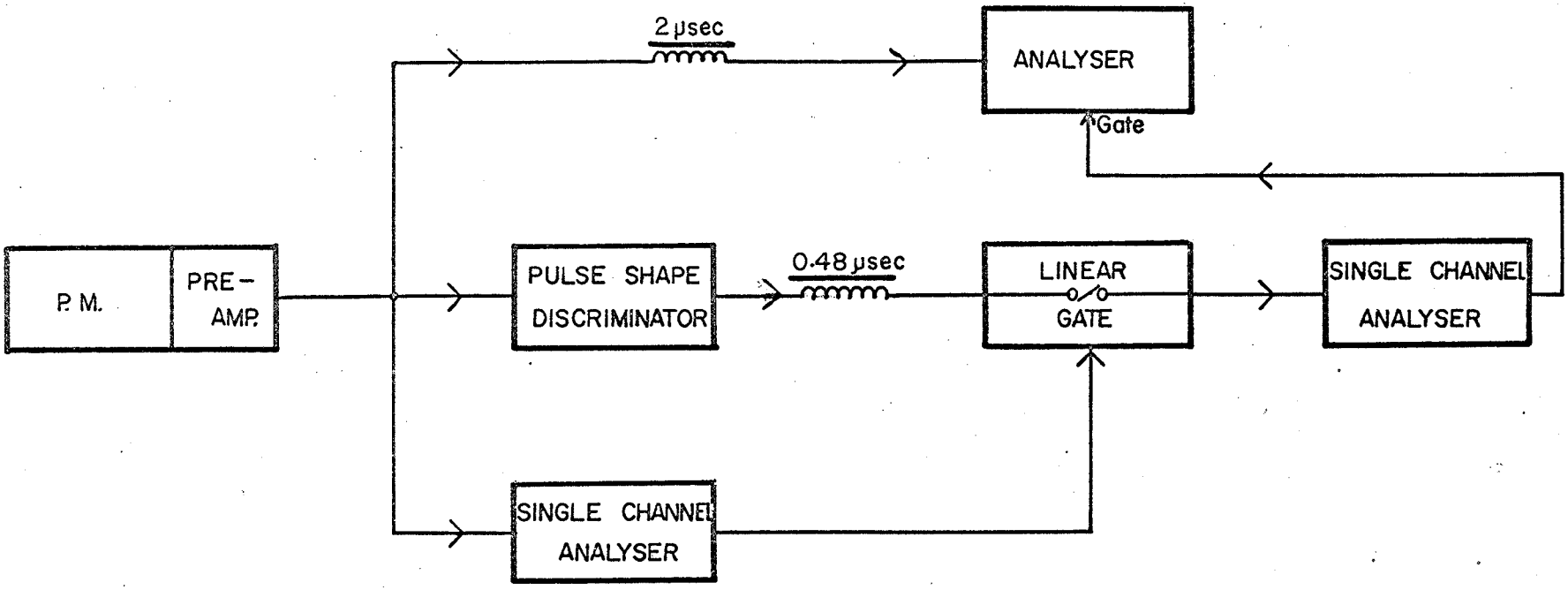
2 μsec
ANALYSER
Gate
P. M.
PRE-
AMP.
PULSE SHAPE
DISCRIMINATOR
0·48 μsec
LINEAR
GATE
SINGLE CHANNEL
ANALYSER
SINGLE CHANNEL
ANALYSER

the range of PSD outputs corresponding to a given type of particle. A multichannel analyser was gated by the output from the second SCA, and could thus be used to obtain the spectrum of one type of particle in the presence of other particles.

2.2 Experimental Results

From fig. 8, the pulse shape discriminator output for a given type of particle is constant in the pulse height range 1.6 to 4.6 volts. This gives a dynamic range of 3 to 1. Accordingly, the first SCA of the spectrometer arrangement (fig. 9) was set to accept pulses in this range. Different parts of the energy spectrum were analysed by varying the high voltage applied to the phototube.

Fig. 10(a) shows the direct PSD spectrum obtained with the Am^{241} and Co^{56} sources. The high voltage was such that the pulse height range accepted corresponded to the energy range 0.8 to 2.2 Mev. If the second SCA selected all pulses with a measured zero-crossing time less than 210 nsec. as being alpha-induced pulses, this would result in a 97% acceptance of actual alpha pulses with a gamma rejection of 99.3%. At higher energies the resolution of the two peaks improves, since statistical fluctuations in pulse shape are less, and better discrimination is achieved between alpha- and gamma-induced pulses.

Fig. 10(b) shows a portion of the ungated Am^{241} spectrum, and the gated spectra obtained with either an

FIGURE 10.

(a) PSD spectrum with both the Am^{241} and Co^{56} sources present.

(b) Ungated energy spectrum of the Am^{241} source, together with the gated spectra obtained in coincidence with either an alpha- or gamma-identifying signal.

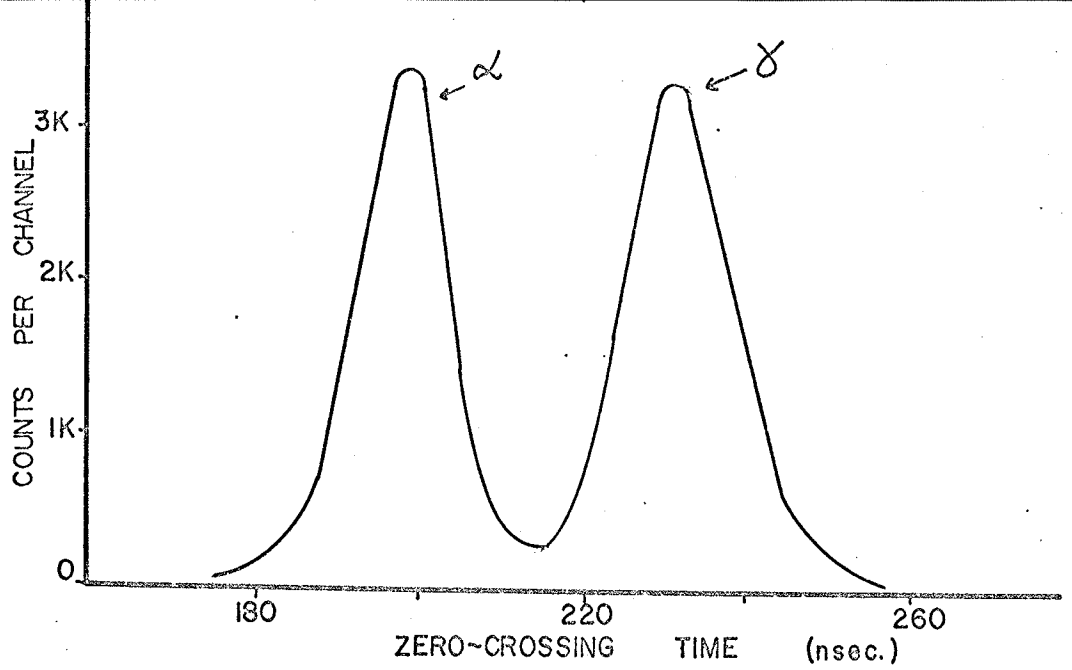
α
γ
3K
2K
1K
0
COUNTS PER CHANNEL
180
220
260
ZERO-CROSSING TIME (nsec.)

(a)

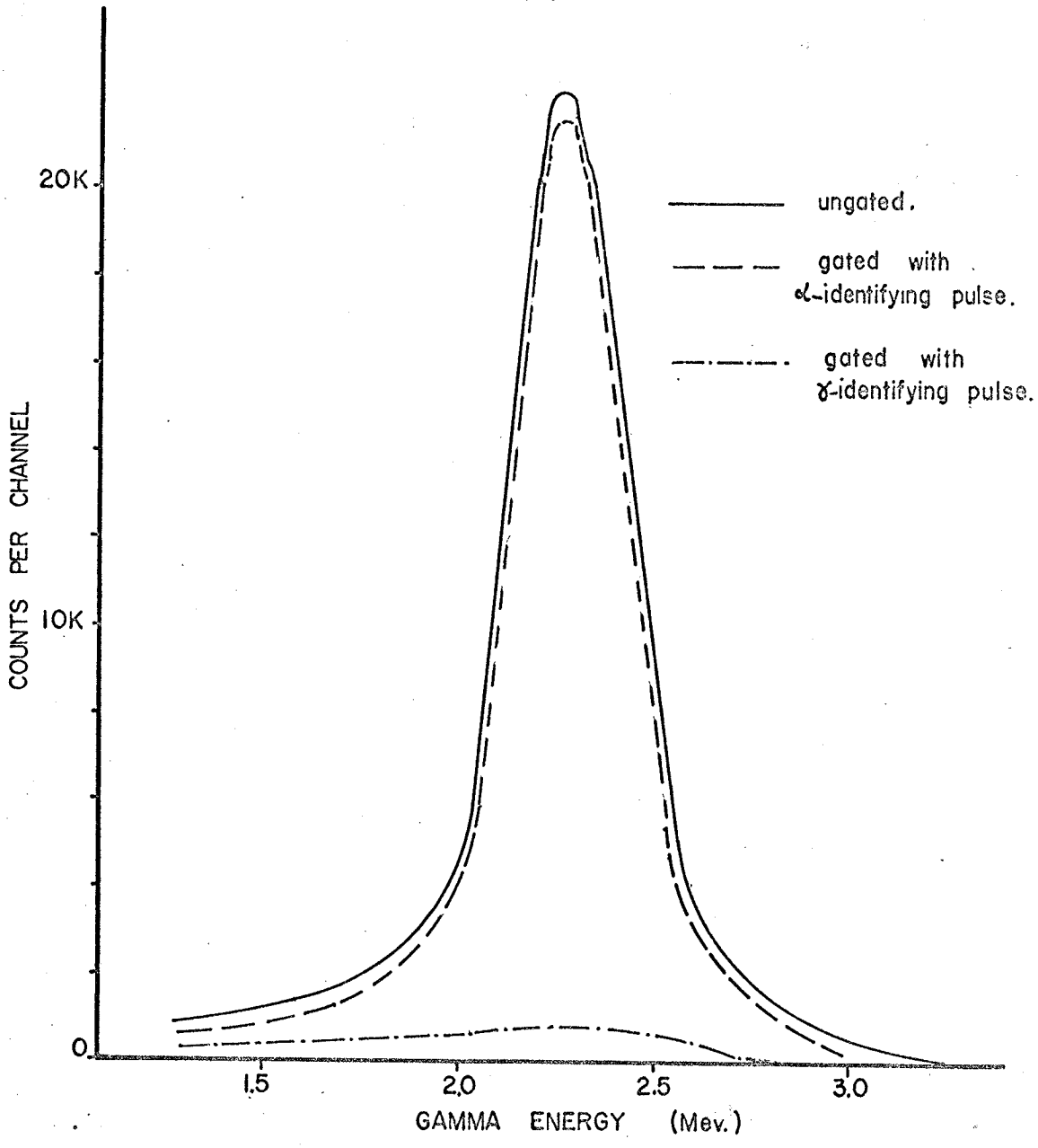
20K
10K
0
COUNTS PER CHANNEL
ungated.
gated with α-identifying pulse.
gated with γ-identifying pulse.
1.5
2.0
2.5
3.0
GAMMA ENERGY (Mev.)

(b)

alpha or a gamma identifying signal. In this case, all pulses with measured zero-crossing times less than 216 nsec. were identified as alpha-induced pulses, and all pulses with measured zero-crossing times greater than 216 nsec. were identified as gamma-induced pulses. Not all alpha-induced pulses were suppressed in the energy spectrum obtained with the multichannel analyser gated by a gamma-identifying signal. Due to statistical fluctuations, more than 1% of the alpha pulses have measured zero-crossing times greater than 216 nsec.

Fig. 11(a) shows the direct PSD spectrum of a Mn^{54} gamma source. The peak at 300 nsec. is pulse distortion due to pile-up. Decreasing the counting rate caused a relatively greater reduction of that peak compared with the true gamma peak at 230 nsec.

Fig. 11(b) shows the 0.84 Mev. gamma peak from Mn^{54}, together with the energy spectra obtained with the analyser accepting only pulses with zero-crossing times either longer or shorter than 272 nsec. The pile-up pulses have a broad peak at a higher energy than the main peak. In this case, only about 85% of the undistorted gamma pulses are accepted by the system, due to dead-time effects in the single channel analysers.

Fig. 12 shows the neutron cross sections for the (n,α), (n,γ), and (n,p) reactions on Na^{23} and I^{127}. No data were found on the cross sections for the $I^{127}(n,\alpha)$ and $I^{127}(n,p)$ reactions at neutron energies below 12 Mev. The cross sections for inelastic scattering of neutrons are not

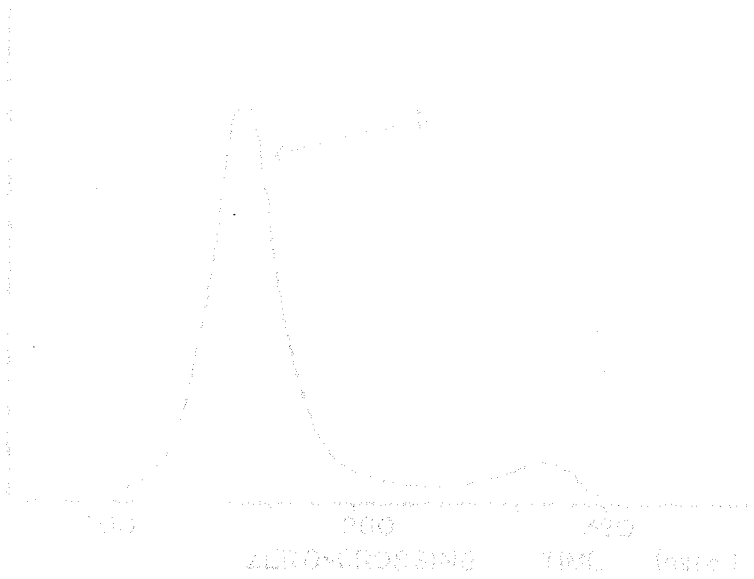

FIGURE 11

(a) PSD spectrum of Mn^{54} at a high counting rate.

(b) Ungated energy spectrum showing the 0.84 Mev. gamma peak from Mn^{54}, together with the gated spectrum obtained in coincidence with a gamma-identifying signal. Also shown is the spectrum of the rejected pulses.

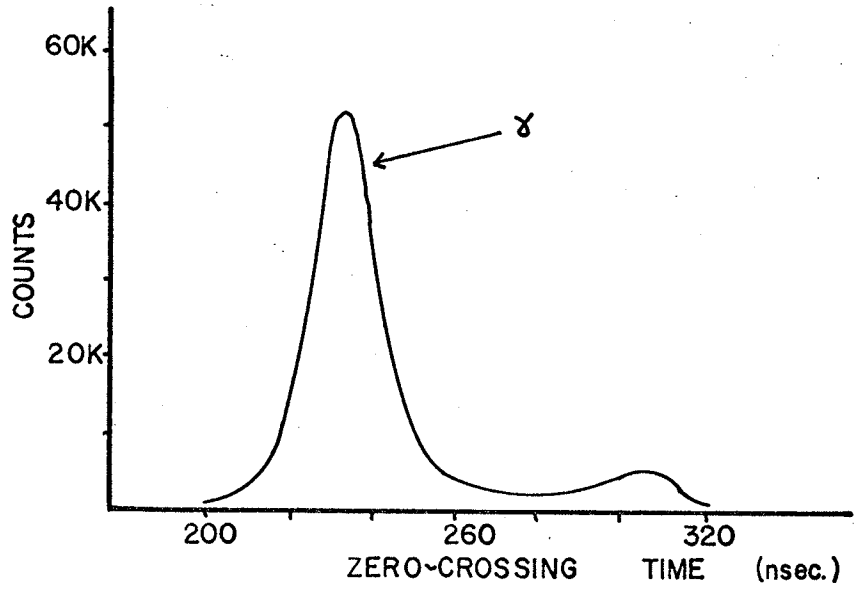
60K
40K
20K
COUNTS
γ
200
260
320
ZERO-CROSSING TIME (nsec.)

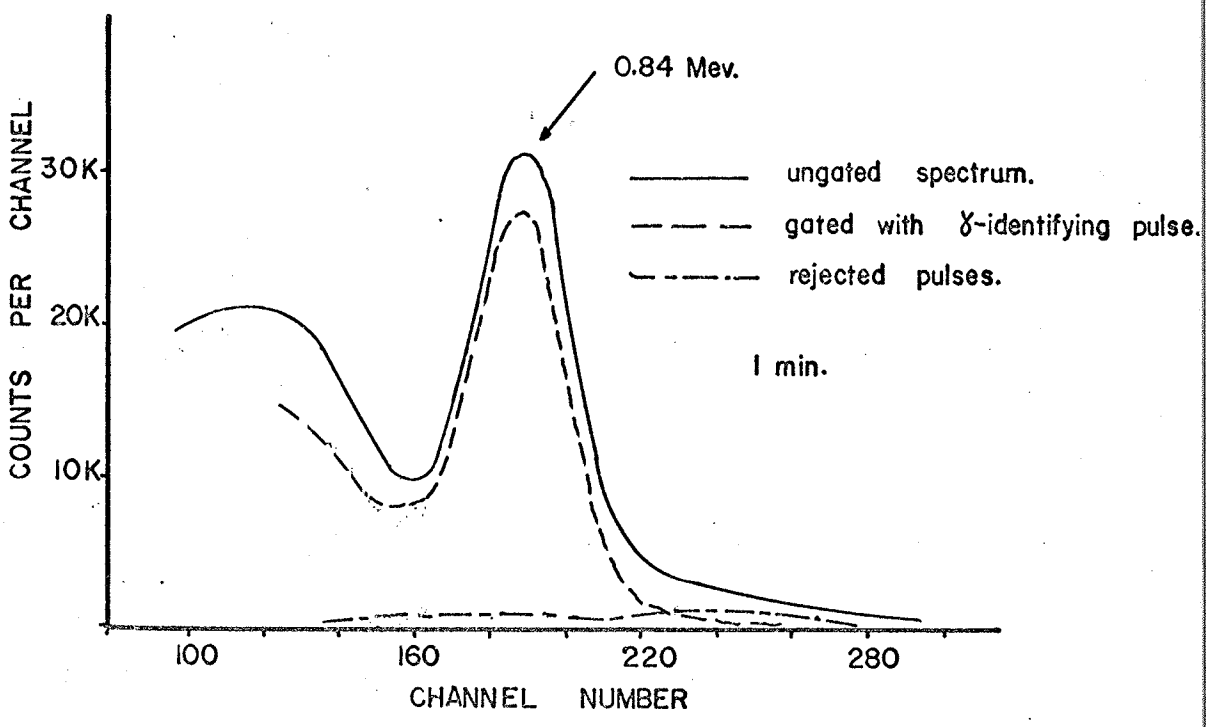
0.84 Mev.
30K
20K
10K
COUNTS PER CHANNEL
ungated spectrum.
gated with γ-identifying pulse.
rejected pulses.
1 min.
100
160
220
280
CHANNEL NUMBER

FIGURE 12.

Neutron cross sections for the (n,α), (n,p), and (n,γ) reactions on Na^{23} and I^{127} for neutron energies from 1 to 20 Mev.
(From BNL325 (1966)).

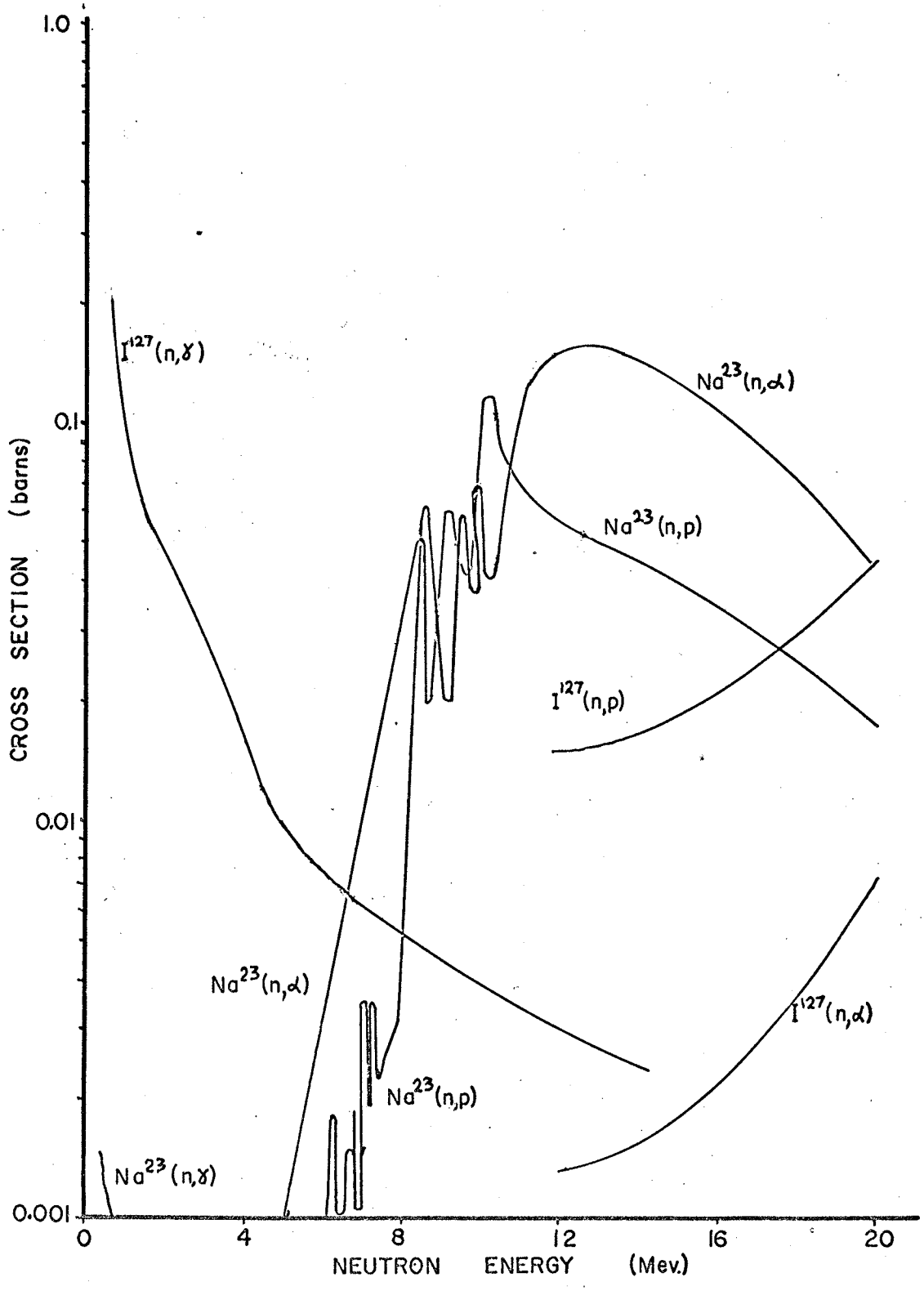
1.0
0.1
0.01
0.001
CROSS SECTION (barns)
$I^{127}(n,\gamma)$
$Na^{23}(n,\alpha)$
$Na^{23}(n,p)$
$I^{127}(n,p)$
$Na^{23}(n,\alpha)$
$Na^{23}(n,p)$
$I^{127}(n,\alpha)$
$Na^{23}(n,\gamma)$
0
4
8
12
16
20
NEUTRON ENERGY (Mev.)

shown. Other possible reactions are reactions yielding more than one particle, which generally have high thresholds and small cross sections at neutron energies below 20 Mev. (for example, the Na^{23} (n, nα) reaction).

The neutron source available was a Cf^{252} fission source emitting a total of 4.10^3 neutrons per second. Fig 13(a) shows the neutron energy spectrum from Cf^{252}. It was calculated that the source, placed axially 2 inches from the cylindrical NaI(Tl) crystal, would give approximately four $Na^{23}(n,\alpha)$ and three $Na^{23}(n,p)$ reactions per second.

The energy spectrum of alpha particles from $Na^{23}(n,\alpha)$ and $I^{127}(n,\alpha)$ reactions for 14 Mev. neutrons has been given by Bizzeti, Bizzeti-Sona, and Bocciolini (1962). The alpha spectrum exhibits a fairly broad peak at about 4 Mev. From these results, the alpha spectrum from the $Na^{23}(n,\alpha)$ reaction with neutrons from the Cf^{252} source should have a peak below 1 Mev. However, attempts to obtain direct PSD spectra showing the presence of alpha-induced scintillations in the energy range 0.4 to 1.0 Mev. were unsuccessful. Although a one inch thickness of lead was placed between the source and the crystal to absorb gamma-rays emitted from the source, the PSD spectrum (see fig. 13(b)) consisted of a single peak at 233nsec., indicating the presence of a large number of gamma-induced scintillations (from inelastic scattering and (n,γ) reactions). This peak was broad (due to the large statistical fluctuations in the pulse shape at low energy) and would completely mask the presence of the relatively small alpha peak expected from our calculations, if indeed such a peak were present. No

FIGURE 13.

(a) Neutron energy spectrum from Cf^{252}. (Calculated from data given by Meadows (1967)).

(b) PSD spectrum for Cf^{252} in the energy range 0.4 to 1.0 Mev.

(c) PSD spectrum for Cf^{252} in the energy range 3 to 8 Mev.

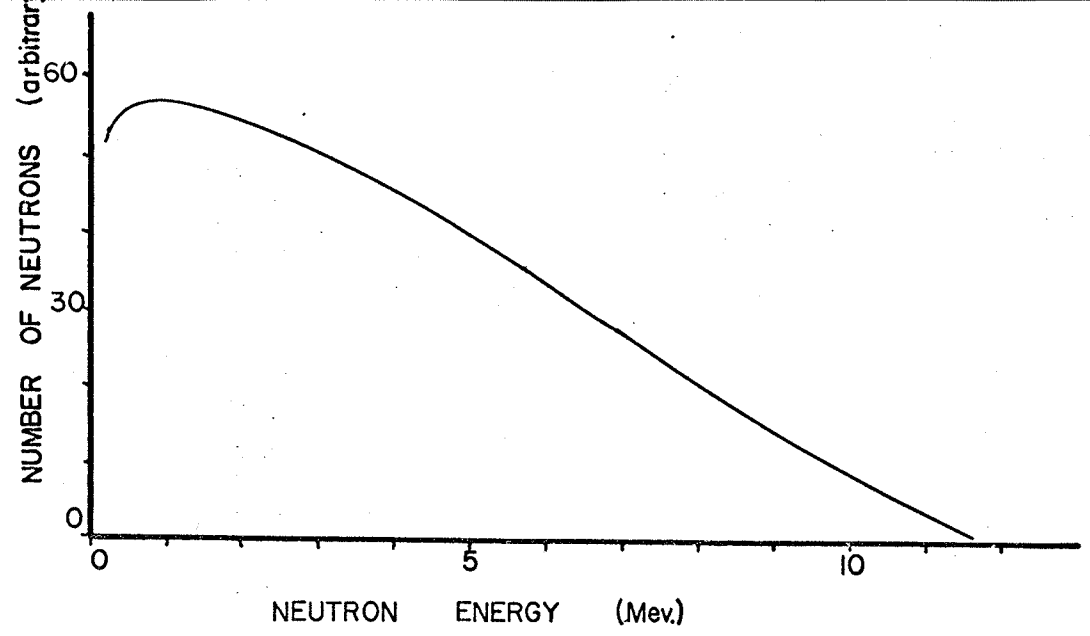
NUMBER OF NEUTRONS (arbitrary)
60
30
0
0
5
10
NEUTRON ENERGY (Mev.)

(a)

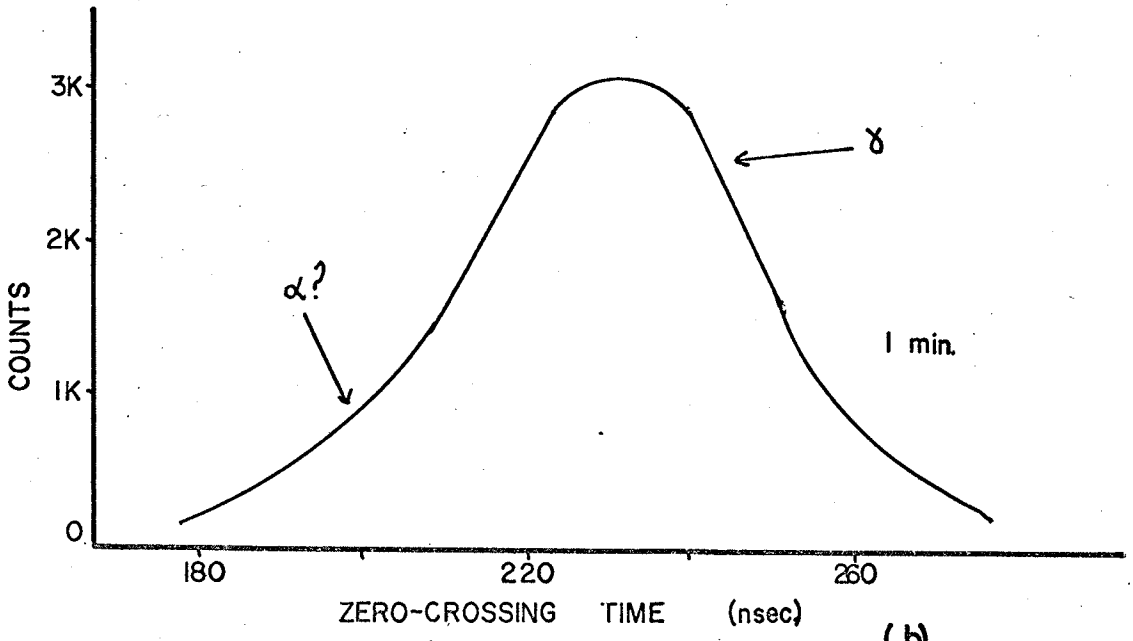
3K
2K
1K
0
COUNTS
γ
α?
1 min.
180
220
260
ZERO-CROSSING TIME (nsec)

(b)

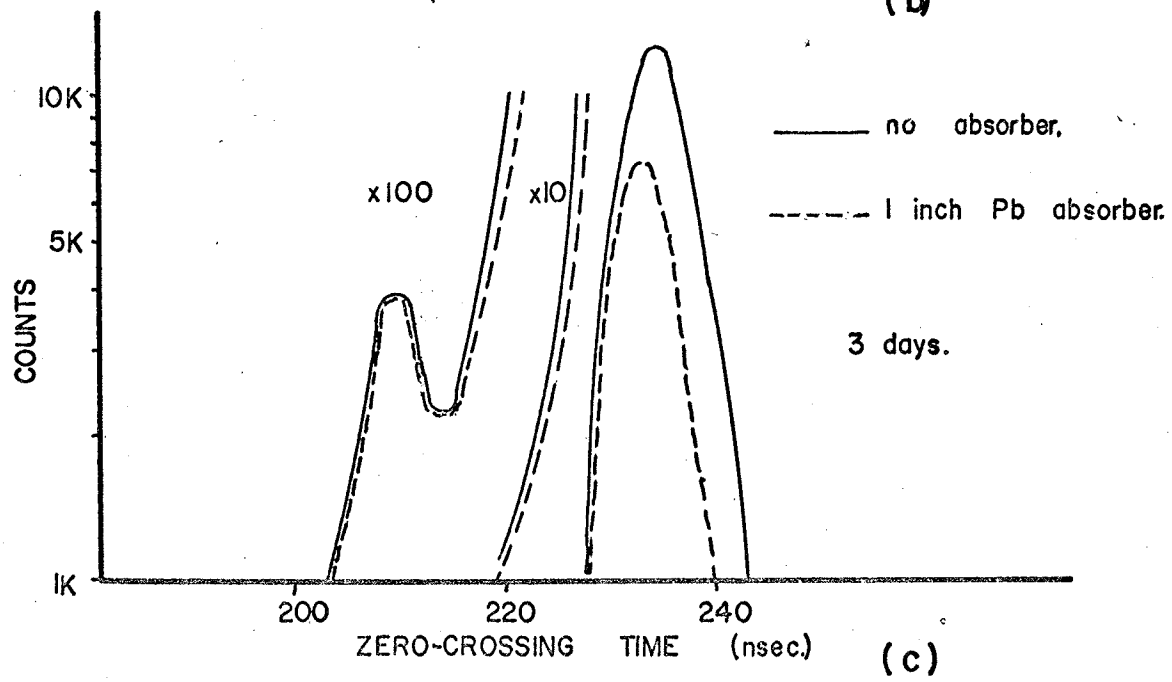
10K
5K
1K
COUNTS
x100
x10
no absorber.
1 inch Pb absorber.
3 days.
200
220
240
ZERO-CROSSING TIME (nsec.)

(c)

significant peak corresponding to alpha-induced pulses was found in PSD spectra for energy ranges up to 3 Mev.

Fig. 13(c) shows the PSD spectrum obtained in the gamma-energy range 3 to 8 Mev. The small peak at 209 nsec. was not reduced by placing one inch of lead between the source and the crystal, while the gamma peak at 233 nsec. was reduced by a factor of two. The peak at 209 nsec. is probably due to proton-induced scintillations arising from the I^{127} (n,p) reaction (Q = +0.1 Mev.) which would be expected to yield protons in that energy range. The very low counting rate made it impractical to obtain an energy spectrum of the pulses with measured zero-crossing times less than 215 nsec.

An alternative source of neutrons was the large neutron flux produced in and around the (p,2p) experimental chamber during operation of the 50 Mev. proton cyclotron at the University of Manitoba. However, direct PSD spectra obtained in energy ranges up to 20 Mev. gave only the characteristic gamma peak and failed to show any significant peaks corresponding to either alpha- or proton-induced scintillations. This is attributed to the large flux of high energy gamma-rays from all directions, and to the presence of large numbers of neutrons with energies below 5 Mev. being inelastically scattered or giving rise to (n,γ) reactions on Na^{23} and I^{127}.

CHAPTER III

CONCLUSIONS.

The main problem which arises in pulse shape discriminators of the zero-crossing type, used with alkali halide scintillators, is the walk with amplitude due to the finite threshold of the leading edge and zero-crossing discriminators. This walk occurs with all published circuits, but does not lead to serious difficulties with most organic and some inorganic scintillator pulses, which generally have fast rise and decay times and considerable differences in pulse shapes for different incident particles. With alkali halide scintillators, the differences in pulse shape for different incident particles are much less, and to make the most efficient use of this information requires the use of long integrating and differentiating time constants. The differentiated pulses then have smaller slopes at the zero-crossing point which not only leads to uncertain firing of the tunnel diode, but also means that a small change in amplitude produces a large walk in the measured zero-crossing point. This is a serious problem with small pulses; with large pulses this walk can be offset to some extent by walk in the leading edge discriminator.

In circuits with just the leading edge and zero-crossing discriminators, the threshold settings of these discriminators can be used to eliminate noise pulses. However, small pulses just above the threshold will trigger the discriminators. Usually the zero-crossing times of such pulses are inaccurately measured, due to uncertain and delayed firing of the tunnel diodes.

The circuit given by Souček and Chase (1967) includes an additional amplitude discriminator to reject small pulses. The leading edge and zero-crossing discriminators are normally biased off, and are unbiased by a signal derived from the amplitude discriminator. However, with the circuit used in the present study, it has been found necessary to set the threshold of the leading edge and zero-crossing discriminators at over 100mv., thus destroying the advantages of this arrangement. The high threshold settings are necessary because of the dc coupling between the tunnel diodes. Souček and Chase (1967) do not state the threshold settings used with their unit. However, threshold settings up to 100mv. would not seriously affect measurement of the zero-crossing times of pulses with fast rise and decay.

The circuit given by Johnson (1968) has only leading edge and zero-crossing discriminators, whose thresholds could be set at 20mv. This would appear to be as low as is practical with tunnel diode discriminators. This circuit would probably give very good discrimination with pulses from a NaI(Tl) scintillator if the differentiated pulses were amplified so that the slopes at the leading edge and zero-crossing points were considerably increased. It does not matter if this amplified pulse is allowed to limit, as with the circuit of Roush, Wilson, and Hornyak (1964). Small pulses could best be eliminated by a diode gate at the input of the pulse shape discriminator, controlled by a discriminator in parallel with the limiting amplifier (see fig. 14). This arrangement would

FIGURE 14.

Block diagram of proposed particle identification system for NaI(Tl) scintillators.

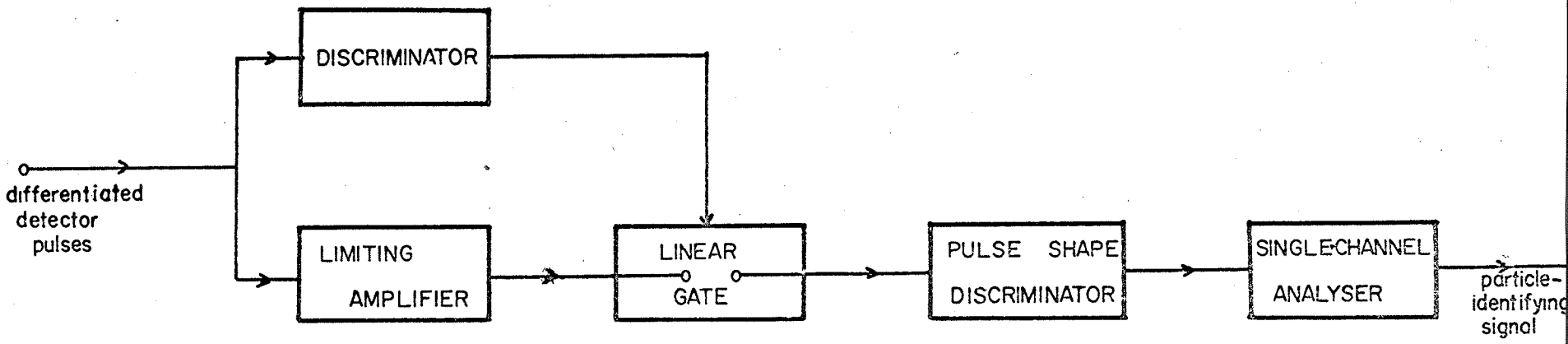
DISCRIMINATOR
differentiated
detector
pulses
LIMITING
AMPLIFIER
LINEAR
GATE
PULSE SHAPE
DISCRIMINATOR
SINGLE-CHANNEL
ANALYSER
particle-
identifying
signal

be more suitable than the circuit given by Souček and Chase (1967) because interaction between the tunnel diodes is reduced to a minimum, and it would practically eliminate the time-slewing with amplitude due to the finite trigger levels of the discriminators. In addition, the limiting amplifier would allow the use of longer integrating and differentiating time constants to optimize the discrimination available with a NaI(Tl) scintillator.

REFERENCES

Bass, R., W. Kessel and G. Majoni, 1964, Nucl. Instr. Meth. 30, 237

Batchelor, R., W. B. Gilboy, A. D. Purnell and J. H. Towle, 1960, Nucl. Instr, Meth. 8, 146.

Bizzeti, P. G., A. M. Bizzeti-Sona and M. Bocciolini, 1962 Nucl, Phys. 36, 38.

BNL 325, 1966, "Neutron Cross Sections".

Brooks, F. D., 1956, Prog. Nucl. Phys. 5, 252.

Brooks, F. D., R. W. Pringle and B. L. Funt, I.R.E. Trans. Nucl. Sci. NS-7, (2-3), 35.

Chaminade, R., J. C. Faivre and J. Pain, 1967, Nucl. Instr. Meth. 44, 217.

Forte, M., 1959, Studia Ghisleriana 4, 281.

Forte, M., K. Konsta and C. Maranzana, 1961, Proc. Conf. Nucl. Electronics, Belgrade, 277.

Fulle, R., Gy. Mathe and D Netzband, 1965, Nucl. Instr. Meth. 35, 250.

Goulding, F. S., D. A. Landis, J. Cerny and R. H. Pehl, 1964, Nucl. Instr. Meth. 31, 1.

Hiramoto, T., Y. Noda and T. Mizutani, 1967, Nucl. Instr. Meth. 46, 261.

Hiramoto, T. and N. Nohara, 1968, Nucl. Instr. Meth. 58, 167.

Johnson, F. A., 1968, Nucl. Instr. Meth. 58, 134.

Jones, D. W., 1968, Nucl. Instr. Meth. 62, 19.

Legler, E., W. Attwenger, F. May and C. Quittner, 1965, Rev. Sci. Instr. 36, 1167.

Máthé, Gy., 1966, Nucl. Instr. Meth. 39, 356.

Máthé, Gy., and B. Schlenk, 1964, Nucl. Instr. Meth. 27, 10.

Meadows, J. W. 1967, Phys. Rev. 157, (4), 1076.

Nadav, E. and B. Kaufman, 1965, Nucl. Instr. Meth. 33, 289.

Owen, R. B., 1958, I.R.E. Trans. Nucl. Sci. NS-5. (3), 198.

Owen, R. B. 1962, I.R.E. Trans. Nucl. Sci. NS-9, (3), 285.

Roush, M. L., M. A. Wilson and W. F. Hornyak, 1964, Nucl. Instr. Meth. 31, 112.

Sabbah, B. and A. Suhami, 1968, Nucl. Instr. Meth. 58, 102.

Souček, B. and R. L. Chase, 1967, Nucl. Instr. Meth. 50, 71.

Turos, A. and A. Zieminski, 1966, Nucl. Instr. Meth. 44, 119.

Wall, W. R. and K. I. Roulston, 1968, to be published.

Wolfe, B., A. Silverman and J. W. DeWire, 1955, Rev. Sci. Instr. 26, (5), 504.